Diss. ETH No 12424

Degradable, Tubular DegraPol®-Implants

A dissertation submitted to the

Swiss Federal Institute of Technology Zurich

for the degree of
Doctor of Technical Sciences

presented by

Rémy Cédric Stoll

Dipl. Werkstoff-Ing. ETH
DEA, Univ. Paris VI
born October 16, 1968
Place of origin: Schaffhausen and Osterfingen SH

accepted on the recommendation of
Prof. Dr. Ulrich W. Suter, examiner
Prof. Dr. David F. Williams, co-examiner
Dr. Peter Neuenschwander, co-examiner

Zurich, 1997

Dinge sind,
was man aus ihnen macht.

Kanzelspruch

First of all, I would like to express to Prof. U.W. Suter and Dr. P. Neuenschwander my gratitude for having entrusted me with one of their very exciting research projects. I greatly appreciated all kinds of support they were giving and the liberty they were offering. Their critical comments made me often think twice, and helped a lot keeping the project on a good way. The enthusiastic interest, they also showed, was always encouraging.

To Prof. D.F. Williams I am grateful for accepting to be my co-examiner in the defence of this thesis.

Many thanks belong also to Prof. P. Aebischer. He actually initiated the DegraPol®-nerve guidance channel project and always was a highly valuable partner with his expert knowledge on nerve regeneration. I shared many good moments with his assistant, Dr. M. Borkenhagen, who carried out the animal testing of the implants. His constructive collaboration was decisive for the fruitful development of the project.

I could always rely on the extraordinary technical skills of U. Krebs, M. Wohlwend and H. Seinecke. I wish to thank them for their help and for the construction of all special laboratory equipment I needed.

I would also like to thank:

- J. Friedrich, N. Stingelin, Ph. Kern, and S. Ulrich, who carried out some of their student-projects in the framework of my thesis.

- M. Colussi, F. Bangerter, and D. Sutter for their technical help, support and service measurements in the experimental techniques.

- Dr. P. Walther for Scanning Electron Microscope training and support.

- Dr. B. Saad for the biological investigations.

- All former collaborators of the group, who initiated and continued the DegraPol®-research.

- All friends from the laboratory, that contributed to the beautiful atmosphere.

- thank you!

The following papers and presentations report the main results obtained in the work described in this thesis:

Publications

"Synthesis and Characterization of DegraPol® for Nerve Guidance Channels", R. C. Stoll, P. Neuenschwander, M. Borkenhagen, P. Aebischer, U. W. Suter, in preparation

"Processing of DegraPol® to Tubular Implants for Medical Use", R. C. Stoll, S. Matter, P. Kern, P. Neuenschwander, U. W. Suter, in preparation

"In Vivo Performance of New Biodegradable Polyesterurethane System Used as a Nerve Guidance Channel", M. Borkenhagen, R. C. Stoll, P. Neuenschwander, U. W. Suter, P. Aebischer, *Biomaterials*, submitted

Presentations

Polymer Gruppe Schweiz (PGS), 1996, Fall Meeting Basel Switzerland, oral presentation "Thermoplastic Elastomers as Biocompatible Materials; DegraPol® as an Example", R.C. Stoll, A. Lendlein, P. Neuenschwander, U.W. Suter

Swiss Society of Biomaterials (SSB), 1997, annual meeting in Lausanne, Switzerland, oral presentation "Performance of DegraPol® as Nerve Guidance Channels", R.C. Stoll, P. Neuenschwander, U.W. Suter and M. Borkenhagen, P. Aebischer

European Physical Society (EPS), 1997, Lausanne, Switzerland, poster presentation "Processing of DegraPol® to Tubular Implants for Medical Use", R.C. Stoll, S. Matter, P. Neuenschwander, U.W. Suter

Contents

Zusammenfassung

Neue, abbaubare, röhrenförmige Implantate für die Nervenregeneration, aus kürzlich entwickelten Blockcopolymeren (DegraPol®), werden beschrieben. Die Entwicklung dieser Implantate umfasste das Abstimmen der Polymereigenschaften, die Verarbeitung der hergestellten Polymere und das Testen der erhaltenen röhrenförmigen Implantate in einem Tiermodel.

Die verwendeten DegraPol®-Polymere waren aus kristallisierbaren Blöcken, kurzkettigen Polyhydroxybutyrat-Diolen (PHB), und nicht kristallisierbaren Blöcken, Makrodiolen aus Glycolid und ε-Caprolakton, aufgebaut. Die beiden Makrodiol-Typen wurden mit Trimethyl-Hexamethylendiisozyanat zu langkettigen Polymeren polyaddiert. In früheren Untersuchungen hatten sich diese Polymertypen durch ihre gute Zell- und Gewebeverträglichkeit, verbunden mit anpassbaren Abbaugeschwindigkeiten und anpassbaren mechanischen Eigenschaften ausgezeichnet.

Das gewünschte Abbauverhalten der Implantate wurde in folgenden Schritten erreicht:

- Auswahl der nichtkristallisierbaren Blöcke mit geeignetem Abbauprofil.
- Drastische Reduktion der am langsamsten abbauenden Materialkomponenten, der kristallinen PHB-Blöcke im Copolymeren.
- Reduktion des Implantatvolumens durch Optimierung der Röhren-Wandstärke.

Der PHB-Anteil im Polymer konnte nicht beliebig verkleinert werden, da dadurch einerseits die Materialfestigkeit verringert wurde und andererseits die Erstarrungsgeschwindigkeit der frisch extrudierten Polymerschmelze zu langsam wurde.

Aufgrund bekannter Domänenbildungsphänomene bei Multiblock-Copolymeren wurde angenommen, dass eine engere Blocklängenverteilung der PHB-Blöcke die Domänenbildung positiv beeinflussen würde. Zur Steuerung der Blocklängenverteilung wurde eine geeignete fraktionierende Umkristallisations-Methode aus Aceton erarbeitet. Mittels GPC- und ^{1}H-NMR-Analysen konnte nachgewiesen werden, dass diese Methode rein molmassenselektiv war. Die aus Aceton ausgefällte Fraktion enthielt nur noch die oberen 50 % der ursprünglichen Molmassenverteilung; die mittlere Molmasse M_n wurde von 2200 auf 3800 erhöht. Mit diesen umkristallisierten PHB-Diolen konnten Polymere

mit einer mittleren Molmasse von mehr als 100'000 synthetisiert werden. Der PHB-Anteil dieser Polymere wurde bis auf 8 Gew.-% reduziert.

Für die Herstellung der Implantate wurde ein Rammextruder konstruiert, mit welchem kleine Polymermengen (3 - 15 g) kontrolliert und ohne Zusatzstoffe zu dünnen Röhrchen verarbeitet wurden. Durch Optimierung der Extrusionsparameter konnten aus allen synthetisierten Polymeren dünnwandige Röhrchen mit 1.5 mm Innendurchmesser hergestellt werden. Zusätzlich wurden in einem Lösungs-Extrusionsverfahren Röhrchen mit porösen Wänden hergestellt.

Total 26 Nervenregenerationsimplantate mit einem PHB-Anteilen von 41, 17 und 8 Gew.-% wurden in Ratten implantiert und nach 4, 12 oder 24 Wochen untersucht. In 23 Fällen hatte sich im Implantat ein Nervenkabel, bestehend aus myelinisierten Axonen und Schwanzellen, gebildet. Nach 24 Wochen Implantationszeit konnte aufgrund der veränderten chemischen Zusammensetzung der drei verwendeten Implantatmaterialien ein Massenverlust von mindestens 33, 74 und 88 % abgeschätzt werden. Die mikroskopische Erscheinung der am stärksten abgebauten Explantate legte die Vermutung nahe, dass dieses Material nach einem Jahr vollständig resorbiert wäre. Aus dem Vergleich des Abbauverhaltens im Tier mit dem Abbauverhalten in Pufferlösungen konnte für diese Polymertypen ein dreistufiges Abbaumodell vorgeschlagen werden.

Entsprechend ihrem Anforderungsprofil waren die hier entwickelten Implantate während ihrer gesamten Verweilzeit im Körper gut verträglich. Während der ersten vier Einsatzwochen bewahrten die Implantate eine genügende mechanische Festigkeit. Sie stabilisierten die zwei von einander getrennten Nervenenden und hielten dazwischen einen Freiraum offen, bis sich Nervengewebe neu gebildet hatte. Später löste sich das Implantatmaterial zum grossen Teil auf, ohne dabei die Nervenheilung negativ zu beeinflussen.

Diese Resultate sind vielversprechend für die medizinische Anwendung solcher Implantate. Andersweitige medizinische Anwendungen der Polymere sind auch in Betracht zu ziehen.

Abstract

Novel, degradable tubular implants for nerve regeneration, made from recently developed types of cell- and tissue compatible DegraPol® block-copolymers, are described. The implant-development involved the modulation of the polymer, the processing of the synthesized polymers to slender tubes, and the testing of the tubes as nerve guidance channels for rats.

The required grades of DegraPol®-polymers were prepared from non-crystallizable blocks of poly[glycolide-*co*-(ε-caprolactone)]-diol and crystallizable blocks of poly[(*R*)-3-hydroxybutyric acid-*co*-(*R*)-3-hydroxyvaleric acid]-diol (PHB). The two kinds of telechelic macrodiols were chain extended with 2,2,4-trimethyl hexamethylene diisocyanate. In previous studies these kinds of polymers revealed a good cell and tissue compatibility, combined with adjustable degradation rates and also adjustable mechanical properties.

The desired degradation and resorption properties of the implant-material were achieved by:

- choosing a type of non crystallizable block with the desired degradation profile
- drastically reducing the total amount of the slowest degrading parts of the bulk material, the PHB-blocks
- reducing the amount of implanted material by reducing the wall thickness of the implants.

The reduction of the PHB-content of the polymers was limited by the simultaneous loss of mechanical strength and by the reduced solidification rate of the polymer melt after the extrusion.

According to the known behavior of multiblock copolymers, it was presumed that a narrower size distribution of the PHB-blocks would positively influence the segregation into crystalline and amorphous domains. A fractional precipitation procedure from acetone solutions has been elaborated to narrow the block-size distribution of the PHB-blocks. GPC and ^{1}H-NMR analysis of both fractions, the precipitate and the solution, showed that this fractional precipitation method was purely size selective. The 50 wt-% of lowest molar mass of the original molar mass distribution were removed in the

precipitate. The number-average-molar mass was raised from 2200 to 3800. Polymers made from these precipitated PHB-diols could be synthesized with an average molar mass of more than 100'000. The PHB-content was lowered to 8 wt-%.

A plunger extruder has been constructed for the processing of small polymer quantities (3 - 15 g), into slender tubes without any additives. The extrusion parameters could be adjusted, such as to produce tubes with 1.5 mm inner diameter out of all synthesized polymers. A solution-extrusion process was additionally elaborated to produce porous-walled tubes.

A total of 26 tubes, made of polymers containing 41, 17, and 8 wt-% of PHB were implanted into rats for time periods of 4, 12, and 24 weeks. In 23 experiments tissue-cables composed of numerous myelinated axons and Schwan cells had regenerated. After 24 weeks of implantation, a weight loss of at least 33, 74, and 88 % was estimated from the changed chemical composition of the implant material. From its microscopical appearance, the polymer with initial 8 wt-% of PHB could be expected to be completely resorbed after one year of implantation. Comparing these degradation results with results from degradation in buffered water solution, a three step degradation model could be proposed for these materials.

Fitting in with the requirements, the developed implants had a good biocompatibility over the hole period of implantation. They maintained a sufficient strength during the first weeks of implantation to fix the position of the two separated nerve endings and to keep a volume open for the nerve regeneration. Later, the implant material was resorbed to a great part, without adversely influencing the nerve regeneration.

These results are promising for a successful application of the described implants in medicine. Other medical applications should be considered.

CHAPTER 1

Introduction

DegraPol®

Degradable polymers have a high potential for applications in medicine.[1] The demands on such materials may only be fulfilled with completely new materials especially designed for applications in medicine. To be highly useful, these new polymers should combine good processability, good mechanical properties, and reasonable resorption rates with cell and tissue compatibility. In this context, a class of phase-segregated multi-block polyesters[2] and polyesterurethanes,[3] termed DegraPol®, have been developed.

Potential medical applications of DegraPol® are membranes or tubes to protect a healing site, as in the case of nerve guidance channels,[4] three dimensional structures as cell carriers for tissue engineering,[5] drug release systems, or any combination of these applications.[1] The DegraPol®-class of polymers has been found, so far, to have a good cell and tissue compatibility. Their stiffnes is close to that of many body tissues and can be adjusted almost independently of the adjustable degradation rate. Being soluble in many solvents and processable through standard processing routes of thermoplastics, these polymers offer great freedom of implant design, even for large scale production. Their transparency allows far a good control of the operation site. Furthermore, functional groups can be incorporated into the polymer-backbone. These functional anchor-groups can covalently bind several chemical compounds as well as biomolecules to the polymer for a controlled biological or chemical activity of the material surface.[6]

DegraPol® polymers are prepared by co-condensation of two different types of hydroxy-terminated low-molecular-weight polyesters, one being crystallizable ("hard segment"), the other being non-crystallizable and having a glass transition temperature around -30 °C ("soft segment"). As hard segment, low-molecular-weight telechelic α,ω-dihydroxy-poly[(*R*)-3-hydroxybutyric acid-*co*-(*R*)-3-hydroxyvaleric acid] (PHB-diol),[7] was used. Possible soft segments are, e.g., polycaprolactone-diol, Diorez® (a copolyester diol of adipic acid, ethylene glycol, diethylene glycol, and 1,4-butane diol), or a copolyester diol of diglycolide and ε-caprolactone.[8] As chain extenders, aliphatic diisocyanates such as 2,2,4-trimethylhexamethylene diisocyanate, TMDI,[3] or aliphatic acid chlorides such as sebacoyl chloride were used.

The members of the DegraPol®-class of polymers used were degrading hydrolytically "in vitro" and "in vivo" (subcutaneously implanted) within reasonable time periods that were between a few weeks and several months. The degradation consisted in a reduction of molar mass, in the loss of all mechanical resilience such as toughness and high elongation at break, and in some mass loss. However, the PHB blocks in the polymers remained as a solid after degradation and were not resorbed within the observation intervals of some months. They seemed to be stable for a much longer period of time than the aimed degradation and resorption period of several months. This would make it much more difficult to exclude any negative long-term effects of DegraPol®.

A possible way for complete resorption of PHB within the desired period of time of few months is the phagocytosis of PHB-particles by macrophages. In a model study, PHB macromolecules of molecular weight of about 2500, labeled with fluorescent dies, were synthesized and precipitated to form particles in the size range of 10 μm.[9] The phagocytosis and subsequent degradation of these particles could then be followed in cell cultures, and has been found as a possible rapid resorption path (order of 10 days) for PHB-particles.

The reduction of the PHB-content of the copolymers should increase the probability of complete resorption of the material in two ways: first, the quantity of slowly degrading

PHB is reduced, and second, the PHB domains become more isolated in the copolymer, leading more probably to the small PHB particles that can be phagocytosed.

There are two limiting factors for the reduction of the PHB content of the copolymers. On one hand, each copolymer chain should bear at least two PHB blocks to keep the fraction of tangling or lose chains, not contributing to the mechanical stability, low. On the other hand, the copolymers with reduced PHB content should still have the good processability of the DegraPol®-polymers known so far. In fact, the reduction of the PHB content of a DegraPol®/btgc from 41 wt-% to 30 wt-% lead to a drastically reduced solidification rates after extrusion, making this type of processing impracticable.[10]

For the PHB blocks used, the melting point increases with the block length. High molecular weight PHB has been found to form lamellas that are 5 nm to 10 nm thick, corresponding to the length of chains consisting of 15 to 30 hydroxybutyric acid units.[11,12] PHB blocks with lower degrees of polymerization can, therefore, only form lower melting crystalline domains that are forming weaker physical crosslinks within the polymer. Generally the properties of multiblock polyesterurethanes can be improved by narrowing the length distribution of the crystallizable blocks, which leeds to better phase separation and to a higher degree of crystallinity.[13] We therefore surmised that by removing the short blocks from the block-length distribution of the PHB blocks, the mechanical properties as well as the processability of the DegraPol® polymers with low contents of crystallizable blocks could be improved.

To successfully find their way into medical applications, new materials for medicine have to be developed in an interactive process between chemistry, biology and medicine. Simple and flawless implants are needed for this interactive development, to learn more about the material behavior during application. The first application chosen to test the behavior of DegraPol®-polymers were nerve guidance channels used for peripheral nerve regeneration.[4] The most important mechanical requirement on such a channel is to withstand the almost static pressure of the surrounding tissue. Upon completion of regeneration the channel structure no longer serves any purpose. In fact, it may become

detrimental due to mechanical impingement or infection.[14] Besides making secondary surgery unnecessary, biodegradable nerve guidance channels potentially avoid these problems.

Nerve Regeneration

The golden standard of clinical nerve repair procedures consists in the coaptation of both severed nerve endings using fine suture material or by interposing an autologous nerve graft between severed nerve ends in the case of larger nerve defects. Nerve guidance channels (NGCs) are polymeric tubular conduits onto which both severed nerve endings can be sutured. They offer a potential alternative to autograft repair of large nerve defects. In a recent study, collagen-based NGCs were compared to autologous nerve grafts or direct suture repair in a transected median nerve primate model.[15] After 3.5 years no significant difference in behavior, electrophysiology and morphological appearance between each repair technique could be detected.

Besides simplifying suturing procedures and preventing scar tissue ingrowth into the regenerating environment, NGCs can be designed to positively effect the regenerating process. NGCs releasing trophic factors or containing artificial extracellular matrix-like material within their lumen, have been reported to enhance peripheral nerve regeneration.[16,17,18] However, upon completion of regeneration the channel structure no longer serves any purpose. In fact, it may become detrimental due to mechanical impingement or infection.[19] Besides making secondary surgery unnecessary, biodegradable NGCs potentially avoid these problems. Different biodegradable materials have been tested experimentally, such as polyglycolic acid, amorphous copolymers out of D,L-lactic acid and ε-caprolactone and polyurethane-based materials.[20,21,22,23,24,25,26] NGCs have also been fabricated out of biological polymers such as collagen or hyaluronic acid.[27,28] All these polymer systems were accompanied by swelling of the tube's wall which may potentially impede the nerve regeneration process by occluding the channel's lumen. Also, degradation rates were rather slow as the integrity of the channel structure was still preserved after 3 months.[24] The biosafety issue related to animal derived material such as prions from bovine derived collagen and

difficulties in predicting resorption rates also justifies the further investigation of substitute synthetic material for nerve guidance channels.

Thesis Goal

The main purpose of this thesis was to realize a medical application for recently developed DegraPol®-polymers. The application should demonstrate the properties of DegraPol® in a useful practical test. Degradable nerve guidance channels were selected as a first application. There, the required implant properties, the needed processing steps and the medical application seemed to be adequate goals to reach at the current development stage of DegraPol®.

Among recently developed variations of DegraPol®, the most promising members of this family of block-copolymers have to be selected. Degradation studies in buffered water solutions, carried out during the polymer development, are the basis of this selection. The degradation rate should be slow enough to maintain the stability of the nerve guidance channel at least during the first four weeks of implantation. On the other hand, the nerve guidance channel should completely be resorbed within the following couple of months. Neither the degradation nor the resorption of the implanted material should have any negative effects on the host body. DegraPol® degradation is a continuous process and thus the mechanical stability of the implant varies during the implantation period. The required implant properties do also change, as nerve regeneration is going on. In an optimized degradable implant, the degradation rate will be adapted to the regeneration rate of the nerve.

DegraPol®-block-copolymers can be adapted to an application by changing the chemical structure. They can also be adapted by changing the relative amount, the molecular weight, or the molecular weight distribution of the building blocks. The later way shall be used in this study. A series of polymers, containing different relative amounts of crystallizable blocks, shall be synthesized and used in an empirical investigation to optimize the implant properties. Keeping the chemical structure of the used building

blocks the same, the number of parameters potentially influencing the biocompatibility of the implants will be reduced. The same chemical reactions can be used for the synthesis of materials with different mechanical properties and different degradation rates. Polymers with low contents of crystallizable polyhydroxybutyrate-blocks may be of special interest. In former investigations,[29] a bulk material, mainly composed of these crystallizable blocks remained relatively stable after advanced degradation.

A small scale production of implants shall be worked out. This production shall demonstrate the processability of DegraPol®-polymers through standard processing routes of thermoplastics. A plunger extruder seems to be the adequate setup for this purpose. This plunger extruder will have to be designed and constructed to allow the production of nerve guidance channels in a controlled and reproducible way. The extruder should be flexible to allow changes of the nerve guidance channel design. It should have a small dead volume for an efficient processing of few gramms of polymer into slender tubes.

The basic relations between the mechanical properties of the nerve guidance channels, their geometry, and the mechanical properties of the implant material, shall be used to optimize the implant design. Such relations may be deduced from known mechanical properties of linear-elastic materials.

A set of nerve guidance channels shall be used for the regeneration of transected sciatic nerves of rats. The animal testing has to be carried out in close collaboration with a medical research group. The feed-back from this research group shall be used to optimize the nerve guidance channels. Explanted nerve guidance channels have to be carefully investigated to record the chemical degradation and the material disintegration. A way shall be found to estimate the mass loss of the implant, even if it has been fragmented during degradation. The usefulness of the implants shall be demonstrated by the nerve regeneration and by the level of inflammatory reaction, as monitored by the medical research group.

Three open porous dimensional structures and porous-walled tubes may be produced as a

suplement. The three dimensional structures would conect the materials development for nerve guidance channels with the research on DegraPol® structures for tissue engineering.[5] Porous-walled tubes have interesting mechanical properties. They combine a low critical bending radius for kinking with a relatively high tube compliance[31] and may have selective permeabilities for different molecules. They would also demonstrate the broad processing possibilities of DegraPol®.

CHAPTER 2

Polymer Synthesis and Characterization

Introduction

DegraPol®-polymers are biomaterials, developed to cover a broad range of mechanical properties and degradation rates using just few different building units. As multiblock-copolymers the properties are defined by the blocks building up the polymer chains. Changing the relative amount, the size, or the size distribution of the used blocks, different types of polymers can be synthesized using the same chain-extension reaction. The mechanical properties and the degradation profiles can be controlled in that way. As the same type of chemical groups will be present in all such polymers, a similar cell- and tissue-compatibility may be expected.

Based on previous results concerning the degradation profile, the mechanical properties, the cell- and tissue-compatibility, and the ease of chemical synthesis,[3,8] the building blocks to be used for this work have been selected. As crystallizable blocks, low molecular weight PHB-diols have been chosen. As non-crystallizable blocks, random copolymers of glycolide units and ε-caprolactone-units, synthesized as telechelic diols, have been chosen. These diols were chain extended with 2,2,4-trimethylhexamethylene-diisocyanate. To control the size and the size-distribution of the crystallizable PHB-diols, an additional fractional precipitation-step was introduced into polymer preparation. Using fractionated PHB-diols the polymer properties could be improved, particularly at low PHB-contents. A set of such polymers with different amounts of each type of block was used for nerve guidance channels. The best performing material could then be

determined. For the first time, the adaptability of the DegraPol®-family of polymers has been used to meet the requirements of an application.

Results and Discussion

Fractional Precipitation of PHB-Diol

PHB-diol (M_w = 2800) was gradually precipitated from 6 different solvents: ethanol, methanol, dimethyl sulfoxide, diethylene glycol dimethyl ether, acetone, and tetrahydrofurane. The relative amount of PHB that remained dissolved after the precipitation at room temperature varied between 14 % in ethanol and 100 % in tetrahydrofurane, thus the solvents used spaned the entire range of solvent quality. As an indication of the solvent quality, the fraction remaining in solution is plotted against the solubility parameter,[32] δ, in Figure 1. From this data, and assuming that complete dissolution requires a difference in δ between solvent and solute of less than 3 $(MPa)^{0.5}$, the solubility parameter of the PHB-diols is estimated to be around 18 $(MPa)^{0.5}$.

All dissolved fractions were, as expected, of smaller molar masses than the precipitated fractions. Both kinds of fractions, the dissolved and the precipitated ones, had narrower molar mass distributions than the initial PHB-diols. All of the initial higher-molar-mass molecules were found in the precipitated fractions, whereas different amounts of the lower-molar-mass chains remained dissolved. The precipitation in acetone at room temperature (E), or in tetrahydrofurane at 2 °C (F in Figure 2 and in Figure 3), divided the molar weight distributions into two fractions of about equal size. The PHB-diols of these precipitated fractions were found to be best suited for the synthesis of DegraPol® polymers with low contents of crystallizable blocks.

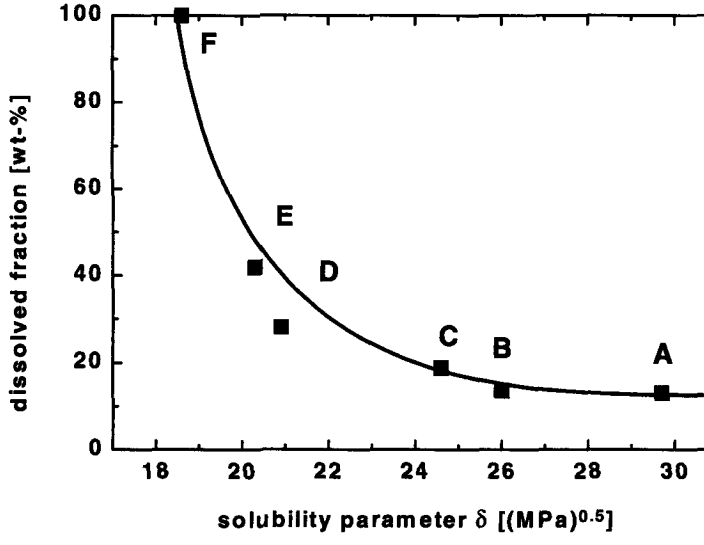

Figure 1 Fraction of PHB-diol remaining in solution in different solvents as a function of the solubility parameter of the solvent (A: ethanol, B: methanol, C: dimethyl sulfoxide, D: diethylene glycol dimethyl ether, E: acetone, and F: tetrahydrofuran).

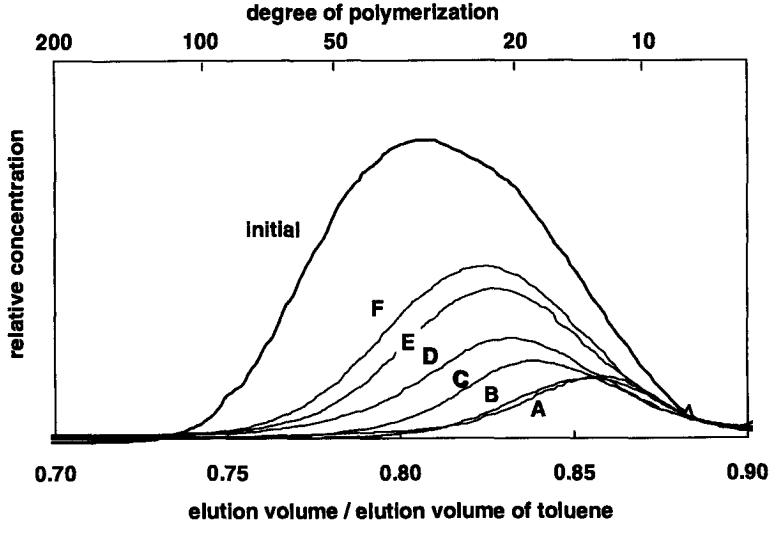

Figure 2 Molecular-weight distributions of the initial PHB-diol and of the fractions remaining dissolved in the solvents indicated (A: ethanol, B: methanol, C: dimethyl sulfoxide, D: diethylene glycol dimethyl ether, E: acetone, and F: tetrahydrofuran at 2 °C). The areas under the curves are proportional to the relative amounts of the fractions (see also Table 1)

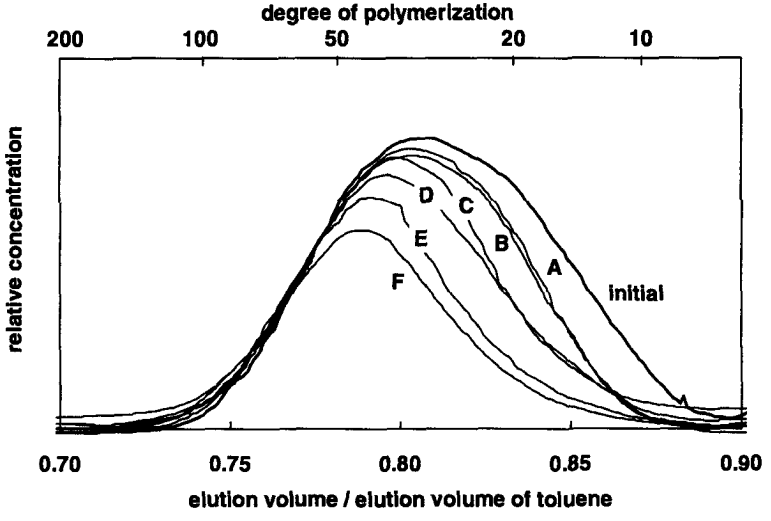

Figure 3 Molecular-weight distributions of the initial PHB-diol and of the fractions precipitated from the solvents indicated (A: ethanol, B: methanol, C: dimethyl sulfoxide, D: diethylene glycol dimethyl ether, E: acetone, and F: tetrahydrofuran at 2 °C). The areas under the curves are proportional to the relative amounts of the fractions (see also Table 1).

The sensitivity of the fractional precipitation with respect to chemical composition, such as the endgroups of the blocks or the content of comonomers (e.g., ethylene glycol units or hydroxyvaleric acid units) was investigated with ^{1}H-NMR. For the most effective molecular-weight selective methods E and F, as reported in Table 1, the precipitated fractions and the fractions remaining in solution did not differ significantly in the relative amounts of the different kinds of end groups. The reactivity of these blocks upon chain extension should therefore not be influenced by the fractional precipitation. Similarly, the content of comonomers in the PHB-diol blocks was not significantly influenced by the fractional precipitation in these separation methods. If it were intended to obtain blocks with as little unreactive end groups as possible, regardless of molecular weight, precipitation from diethylene glycol dimethyl ether would be favorable.

Table 1 Chemical composition of the PHB-diols obtained by fractional precipitation in different solvents.(Precipitation temperature of tetrahydrofuran = 2 °C, all others room temperature)

all units: [%]	endgroups:			ethylene glycol units	hydroxy valerate units
	primary alcohol	secondary alcohol	crotonate	in the PHB chain	
unfractionated PHB-diol (initial)	30	61	9	7	6
fractions precipitated from:					
tetrahydrofuran (F)	29	65	6	7	4
acetone (E)	33	60	7	6	4
diethylene glycol dimethyl ether (D)	87	12	1	1	5
dimethylsulfoxide (C)	35	58	7	6	5
methanol (B)	36	57	7	6	5
ethanol (A)	35	57	7	6	5
fractions dissolved in:					
tetrahydrofuran (F)	40	51	10	6	8
acetone (E)	41	50	9	6	8
diethylene glycol dimethyl ether (D)	51	40	9	5	9
dimethylsulfoxide (C)	37	44	19	6	9
methanol (B)	41	48	11	6	11
ethanol (A)	38	50	12	7	11

Table 2 Properties of the PHB-diol fractions, obtained by fractional precipitation from different solvents. The glass-transition temperatures were measured on quenched samples, the melting points on the precipitated samples.

	relative fraction size	number-average molar mass (VPO)	glass transition (midpoint DSC)	peak melting temperature (DSC)
	[wt-%]		[°C]	[°C]
initial PHB-diol	100	2190	-10	115 / 138
fractions precipitated from:				
tetrahydrofuran (F)	50	-	-3	146
acetone (E)	58	3790	-6	145
diethylene glycol dimethyl ether (D)	72	-	-	130
dimethylsulfoxide (C)	81	-	-23	132
methanol (B)	87	2640	-7	140
ethanol (A)	86	-	-5	140
fractions dissolved in:				
tetrahydrofuran (F)	50	-	-13	128
acetone (E)	42	-	-14	121
diethylene glycol dimethyl ether (D)	28	-	-23	111
dimethylsulfoxide (C)	19	-	-19	119
methanol (B)	13	1060	-24	83
ethanol (A)	14	-	-24	119

Comparing the thermograms of PHB-diol before and after fractional precipitation in acetone, one realizes that the broad multiple-melting endotherms present before fractional precipitation were splitted up. A lower, relatively broad melting endotherm

around 120 °C was mainly found in the dissolved fraction and a higher, relatively sharp melting signal around 140 °C was found in the precipitated fraction, at slightly higher temperature (Figure 4). The absence of the sharp melting signal around 140 °C in the thermogram of the acetone-soluble fraction must be related to higher molar mass PHB-diols, not present in this fraction (as can be seen in Figure 2). The drastically reduced melting signal around 120 °C in the thermogram of the precipitated fraction must be due to the much lower concentration of low molar mass PHB-diols in that fraction (Figure 3). The dependence of the melting point on the molar mass has been described in detail by others.[11,33] The crystalline phase of the precipitated fraction must be rather pure as can be deduced from the sharp melting signal and from the relatively high melting temperature. This could make it suitable as good physical crosslinks in a block copolymer.

Generally, the precipitated fractions had higher average molar mass, narrower molar-mass distributions, higher melting points, higher glass-transition temperatures, and almost the same chemical composition as the initial PHB-diols.

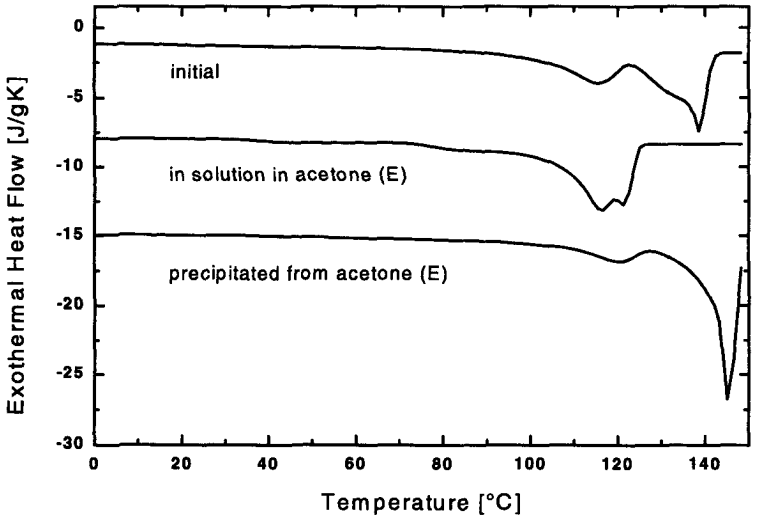

Figure 4 DSC-heating curve of the initial PHB-diol and of the two fractions from the precipitation in acetone.

Soft Segment Synthesis

Poly[glycolide-*co*-(ε-caprolactone)]-diol was prepared by copolymerization of diglycolide and ε-caprolactone by ring-opening polymerization with ethylene glycol.[8] The ratios of reactants were chosen such that the resulting copolymer contained equal amounts of glycolide and ε-caprolactone units, with a resulting number-average molar mass of 2580 (VPO). The composition determined by ^{1}H-NMR is: 29 wt-% glycolide units, 69 wt-% ε-caprolactone units, and 2 wt-% ethylene glycol units. The sequence structure of glycolide and ε-caprolactone units is random (determined by the well-separated ^{1}H-NMR signals of all triads, having a glycolide unit as the center-unit). These soft segments have a glass transition at -43 °C (Figure 5) and no melting point. The soft segment used is, therefore, considered to be liquid and non-crystallizable at ambient temperature. The random copolymerization of diglycolide with ε-caprolactone obviously impedes the crystallization of both of these monomeric units. Poly[ε-caprolactone]-diol was used as purchased.

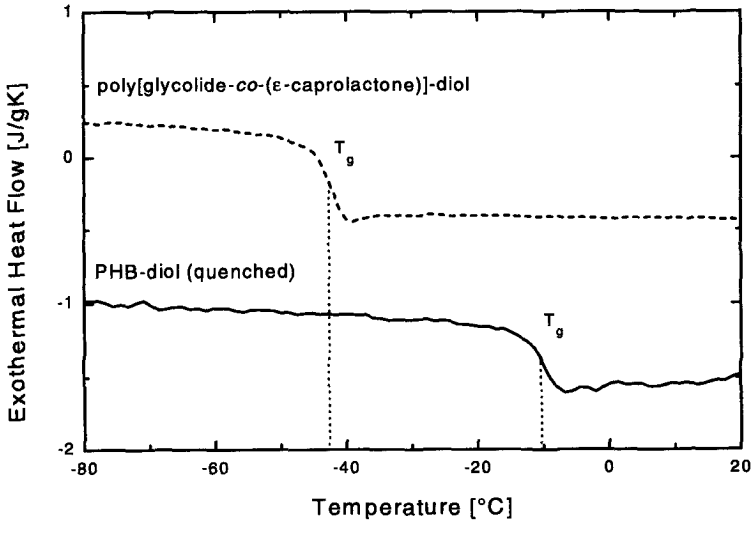

Figure 5 DSC-heating curve of the soft segment employed and of PHB-diol quenched from the melt, showing the glass transition region of both initial building blocks of the polymers described here.

Copolymer Synthesis - Glycolide Containing Polymers

Copolymers were prepared with a target weight ratio of 1:1, 1:4, 1:5, and 1:10 hard to soft segments (Table 3). The three copolymers poorer in PHB, with hard to soft segment ratios of 1:4, 1:5, and 1:10 were prepared with PHB-diol precipitate fraction from acetone, with a number-average molecular weight of about 4000. The copolymer with a hard-to-soft segment ratio of 1:1 was prepared with unfractionated PHB-diol having an number-average molecular weight of 2200. The above described poly[glycolide-*co*-(ε-caprolactone)]-diol was used as a soft segment for all copolymer synthesis and 2,2,4-trimethylhexamethylene diisocyanate was used as a chain extender in equimolar amounts. All but one synthesis yielded in excess of 94 %, after purification and drying (Table 3). GPC-analysis indicated that no starting material remained in the isolated polymers. The copolymer with a ratio of 1:1 was additionally fractionated by precipitation of the polymer from a 2:1 mixture of 1,2-dichloroethane and hexane by

cooling from the boiling point of the solution to room temperature after copolymer synthesis. This additional step increased the average molecular weight and reduced the yield to 80 %. The compositions of the polymers as determined by ^{1}H-NMR are given in Table 4. The weight-average molar masses of all copolymers reached values between 60'000 and 160'000 after synthesis (Table 6).

Copolymer Synthesis - Polymers Without Glycolide

The synthesis method of Hirt, Neuenschwander, and Suter[3] was used for the preparation of the block-copolymers made from soft segments without glycolide units. Polymers were prepared with a target weight ratio of hard to soft segments of 1:1 and 1:2 (Table 3). Unfractionated PHB-diol having a number-average molecular weight of 2200 and poly[ε-caprolactone]-diol (M_n = 1250), as purchased were used as hard and soft segments. 2,2,3-trimethylhexamethylene diisocyanate was used as a chain extender in equimolar amounts.

Table 3 The synthesized block copolymers and their building blocks.

		hard segment		soft segment		synthesis	
polymer name:	target ratio hard segment to soft segment	(PHB)-type	M_n	type	M_n	time [days]	yield [%]
DegraPol®/ btgc b8	1:10	precipitate from acetone	4040	*ran* poly[glycolide-*co*-(ε-caprolactone)]	2580	6	94
DegraPol®/ btgc b14	1:5	precipitate from acetone	4040	"	"	4	97
DegraPol®/ btgc b17	1:4	precipitate from acetone	3840	"	"	6	95
DegraPol®/ btgc b41	1:1	not fractionated (initial)	2190	"	"	56	81
DegraPol®/ btc b45	1:1	not fractionated (initial)	2190	poly[ε-caprolactone]	1250	22	~90
DegraPol®/ btc b29	1:2	not fractionated (initial)	2190	"	"	33	88

Table 4 Chemical composition of the synthesized block copolymers with glycolide containing soft segments, determined by ^{1}H-NMR.

	composition [wt-%]				
polymer name:	hydroxy butyrate/valerate units	hydroxy caproate units	glycolate units	diurethane units	ethylene glycol units
DegraPol®/btgc b8	8	57	27	7	2
DegraPol®/btgc b14	14	53	25	7	2
DegraPol®/btgc b17	17	51	24	7	2
DegraPol®/btgc b41	41	34	15	8	1

Table 5 Chemical composition of the synthesized block copolymers with softsegments containing no glycolide, as in the reaction mixture.

	composition [wt-%]				
polymer name:	hydroxy butyrate/valerate units	hydroxy caproate units	glycolate units	diurethane units	ethylene glycol units
DegraPol®/btc b45	45	45	0	9	1
DegraPol®/btc b29	29	58	0	12	1

Table 6 Molecular and physical properties of the syntesized block copolymers. (n.d. = not determined)

polymer name:	weight-average molecular weight (GPC-LALLS)	glass-transition temperature [°C]	melting point [°C]	Young's modulus [MPa]	yield strength [MPa]	elongation at break [%]
DegraPol® /btgc b8	81'000	-35	122	1.9	0.4	280
DegraPol® /btgc b14	66'000	-35	120	3.7	0.7	320
DegraPol® /btgc b17	62'000	-35	120	8.4	1.1	220
DegraPol® /btgc b41	160'000	-30	123	46	6	1190
DegraPol® /btc b45	~50'000	n.d.	n.d.	n.d.	n.d.	n.d.
DegraPol® /btc b29	~50'000	n.d.	n.d.	n.d.	n.d.	n.d.

Copolymer Properties

Crystalline domains. All wide-angle x-ray diffraction patterns of the copolymers had two characteristic diffraction peaks at diffraction angles of 13.5° (Miller indices: 020)

and 17.0 ° (110), which are typical for crystalline PHB.[34] They could also be found in the diffraction pattern of the not-chain-extended PHB blocks. The intensity of these signals grew as the PHB content of the polymers was increased (Figure 6). Simultaneously, the melting peak integrals at 120 °C in the thermograms increased with growing PHB content (Figure 7). The slight increase in melting temperature with increasing PHB content was probably a crystal-size effect. This is clear evidence that in all these copolymers, low amounts of crystalline PHB domains are present and that the volume fraction increases with the PHB content. A quantitative analysis of the crystallinity shall not be given here, as all the crystalline diffraction signals are relatively small compared to the amorphous halo. Especially at diffraction angles between 20 ° and 25 °, the diffraction peaks of the (021), (101), (111), and (121) crystal planes were not clearly distinguishable from the amorphous signal.

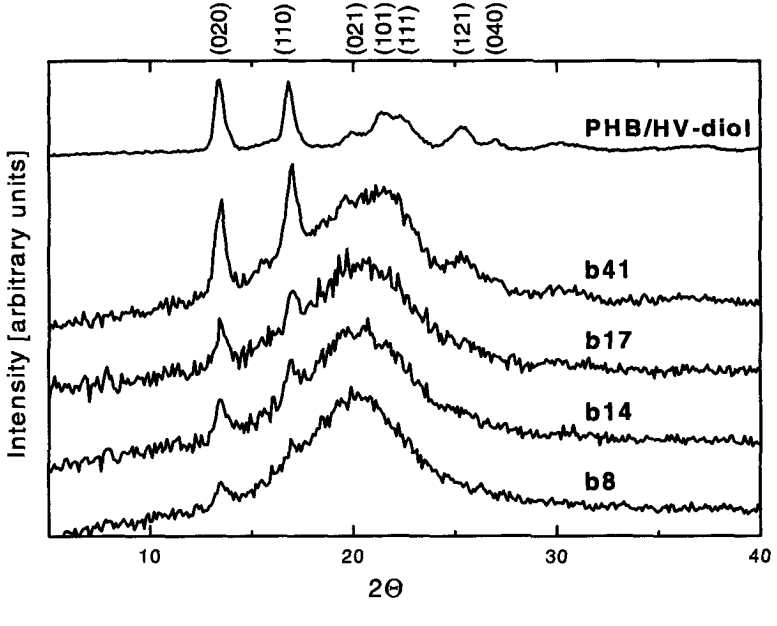

Figure 6 X-ray powder diffraction patterns of the described polymers (DegraPol®/ btgc b8, DegraPol®/btgc b14, DegraPol®/btgc b17, DegraPol®/btgc b41),

and of pure, not chain-extended PHB-diol. The diffraction patterns of the polymers are scaled such that the halo arising from the amorphous domains of the polymers have equal intensities at diffraction angles around $2\theta = 20$ °.

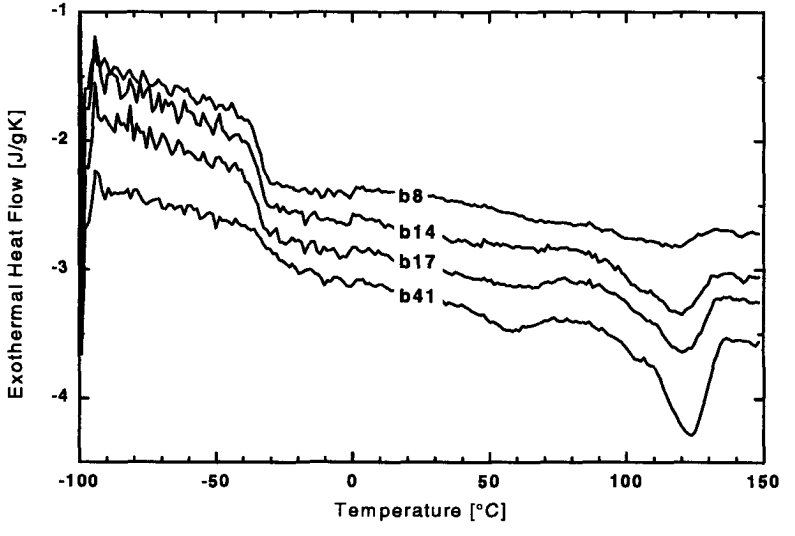

Figure 7 DSC-heating curve of the four described polymers, DegraPol®/btgc b8, DegraPol®/btgc b14, DegraPol®/btgc b17, DegraPol®/btgc b41.

Amorphous domains. The characteristic glass transition signals from the dynamic mechanical measurements at variable temperature of all investigated polymers (single maximum of the loss modulus-curve, Figure 8, step in the storage modulus-curve, Figure 9) indicated that just one kind of homogeneous amorphous domain was present in the polymers. The glass-transition temperatures lied between the glass-transition temperature of the pure, not chain-extended PHB-diol (-10 °C), and that of the soft segment used (-43 °C), but closer to the glass-transition temperature of the pure soft segment (Figure 5 and Figure 8).

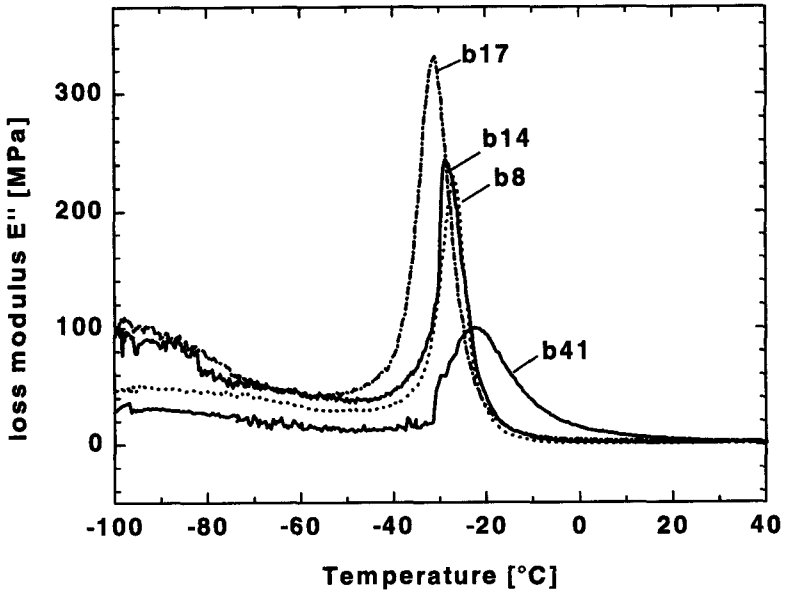

Figure 8 Loss modulus from dynamic-mechanical measurements as a function of temperature for the four described polymers, showing the temperature region of the glass transition. (DegraPol®/btgc b8, DegraPol®/btgc b14, DegraPol®/btgc b17, DegraPol®/btgc b41)

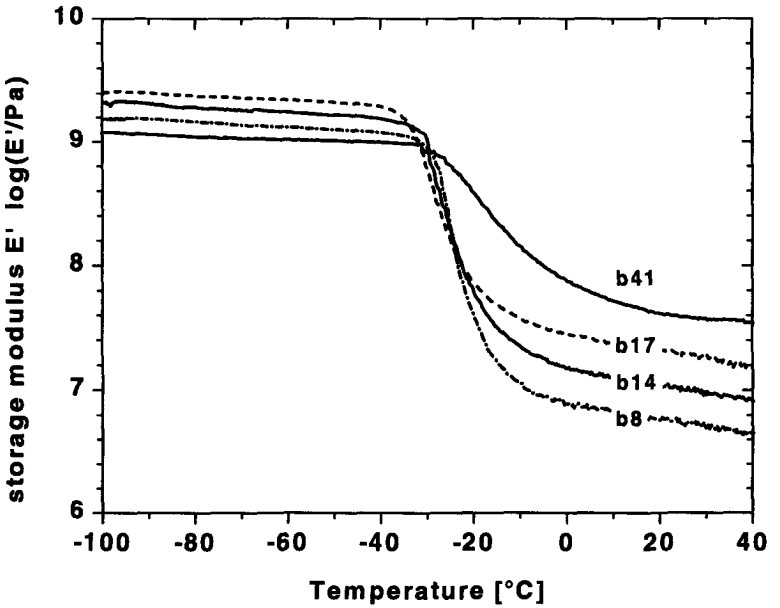

Figure 9 Storage modulus from dynamic-mechanical measurements as a function of temperature for the four described polymers, exhibiting the temperature region of the glass transition. (DegraPol®/btgc b8, DegraPol®/ btgc b14, DegraPol®/btgc b17, DegraPol®/btgc b41)

No transitions could be detected in the temperature range near body temperature, either by DSC or by Dynamic-Mechanical Analysis, and the storage modulus displays no major changes between 0 °C and 50 °C (Figure 9). We conclude that our block copolymers segregate into crystalline PHB domains and into amorphous domains with all soft segment and some PHB.

Mechanical properties. By varying the PHB content in the copolymers, the Young's Modulus has been varied between typical values for elastomers (2 MPa) and for soft thermoplastic polymers (46 MPa). The yield stress of copolymers poor in PHB were quite low, between 0.4 and 1.1 MPa. The elongations at break of more than 250 % were more than was needed for the safe handling and use of the softer copolymers. The

elongation at break of the DegraPol®/btgc b41 of more than 1000 % was extraordinaily high (Figure 10, Table 6).

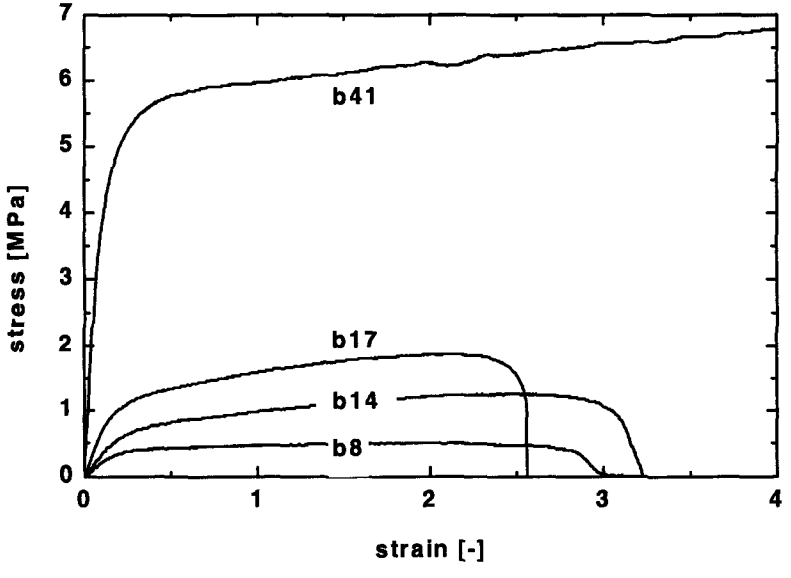

Figure 10 Stress-strain curves from the four described polymers. (DegraPol®/btgc b8, DegraPol®/btgc b14, DegraPol®/btgc b17, DegraPol®/btgc b41); $\dot{\varepsilon} = 0.2s^{-1}$.

The low yield stresses of the polymers reflect their susceptibility to flow. This flow behavior excludes these copolymers from load-bearing applications. Nevertheless, it may be an advantage when an implant should not apply stress to tissue. Implants with this kind of polymer simply release the stress by plastic deformation in such a case. The susceptibility to flow with physically crosslinked, thermoplastic elastomers is generally known, and has also been reported for other such polymers.[35]

The Young's modulus of the tested polymers increased with the content of crystallizable PHB blocks. Considering the block copolymers as mixtures of soft and of hard domains, the increasing Young's modulus could be explained by most of the two phase models,

such as the Takayanagi models,[36] or the model of Gray and McCrum.[37] In these models, the total modulus of a material containing two kinds of domains is a function of the elastic moduli and the fraction of each domain. Considering the block copolymers as Gaussian networks, crosslinked by the crystalline domains, a similar dependence of the total elastic modulus on the PHB content would result as the crosslink density increases with an increasing content of PHB. In rubber networks, often idealized as Gaussian networks, the elastic modulus has been found to depend almost linearly on the crosslink density.[38] It is far beyond the scope of this study to develop a model for the mechanical properties of these polymers; the polymers presented here are with respect to the molar mass distribution of the blocks and of the polymer chains not well-enough defined. However, the elastic modulus can be varied in a broad range with only minor changes of the chemistry of the polymers, but with changes of the hard-/soft-segment ratios.

Contact angles. Advancing contact angles of water between 78 ° and 90 ° were measured on copolymer films cooled from the melt in vacuo and conditioned 7 days subsequently in vacuo. Immersed into water, contact angles of an air bubble were measured between 65 ° and 58 °. (Table 7)

Precipitated polymer, melt-cast polymer films, and extruded tubes of the polymers with the lowest content of PHB (8 wt-%) were tacky. This was probably due their low degree of cristallinity. Immersed into water, the samples became less tacky.

Table 7 Contact angles of an advancing water droplet on the polymer surface and of an air bubble under a horizontal polymer surface in water. The indicated angles are the angles between the polymer-water and the water-air contact areas, the error of the measurement being about ± 5 °.

	contact angle [degrees]	
polymer name:	water in air	air in water
DegraPol®/btgc b8	91	58
DegraPol®/btgc b14	84	65
DegraPol®/btgc b17	82	58
DegraPol®/btgc b41	78	64

Morphology (etched surfaces). Tubes of all four copolymers under investigation, extruded under identical conditions, were etched with methylamine, as described in Chapter 9. In all cases, a structure in the micrometer range was uncovered in this way. The most striking characteristic of these surfaces was the spherulithic structure present only in the DegraPol®/btgc b41. The copolymers DegraPol®/btgc b17, b14, and b8 had a relatively uniform structure covering the entire sample surface, without any nucleation cite visible.

The lamellar structures covering the surfaces of the three copolymers with less PHB were very similar to the lamellar structure spreading radially from the center of the spherulithes in the DegraPol®/btgc b41. The structure seemed to coarsen as the PHB content was reduced. This would suggest, that the spacing between lamellas is increased, the lamellas keeping more or less the same thickness. This tallies with the constant peak width in the WAXD-patterns and with the almost constant melting temperature of the copolymers. DegraPol®/btgc b8 had some particles on the surface that could have been formed by secondary nucleation during the etching process (Figure 11).

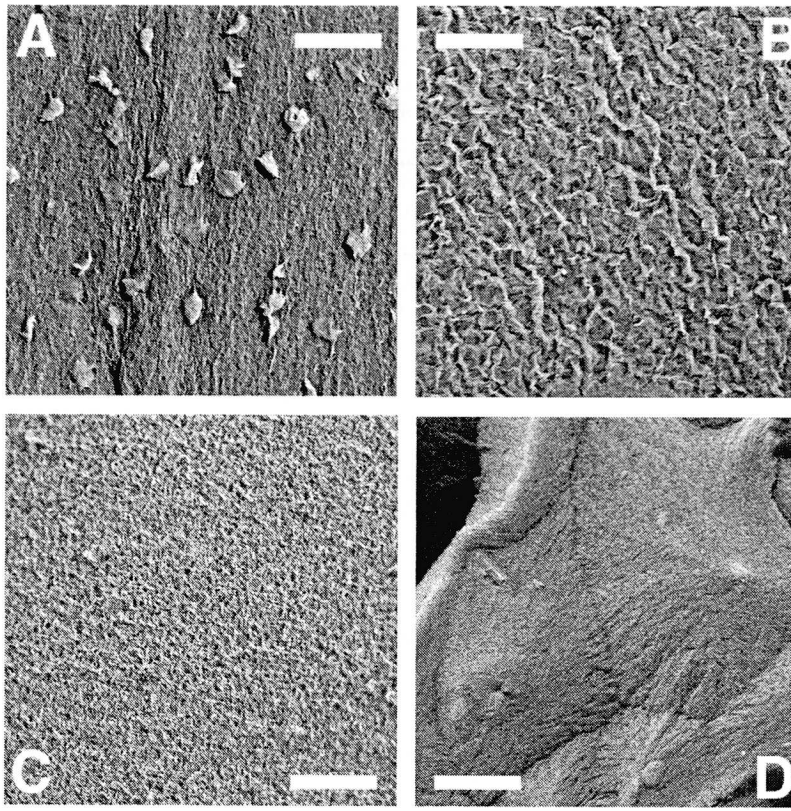

Figure 11 Scanning electron micrographs of etched polymer tube surfaces. A: DegraPol®/btgc b8, B: DegraPol®/btgc b14, C: DegraPol®/btgc b17, D: DegraPol®/btgc b41. Scale bars: 10 µm.

Processability. All polymers could be extruded (without any additives) from their melting into slender tubes with a home-built plunger extruder. The tubes had homogeneous tube walls and smooth inner and outer surfaces. They were soft and highly transparent. They were processed into tubes of well-defined dimensions for a successful use as nerve guidance channels, as will be reported the following chapters. These extruded tubes demonstrate the outstanding processability of these polymers trough

standard processing routes of thermoplastic polymers.

As shown by the data in Table 8, no molecular weight loss occurres during extrusion or compression molding. There was even an increase in molecular weight during the extrusion of the polymers DegraPol®/btgc b8, b14, and b17. A network formation could be excluded as the polymers were still soluble in tetrahydrofurane at 50 °C, as observed during solution preparation for GPC. The true increase in molar mass could be even higher than reported because some parts of the polymer precipitated when the tetrahydrofurane solution was cooled to room temperature and were removed by filtration trough a G4μm glass filter before GPC measurement. Most probably the removed molecules were of higher molar mass than those measured by GPC. Further more, the true concentration of the measured polymer solution was lower than assumed. This lowered again the calculated molar mass average from light scattering measurements as this value is inversly proportional to the concentration of the polymer solution. Over all, the true molar mass of the extruded tube material must be assumed to be up to 50 % higher than the measured values. Possibly, some unreacted isocyanate groups reacted in the extruder with urethane groups, forming allophanates.

Table 8 Molar-mass averages at different steps of polymer processing and sterilization.

	M_w (GPC-LALLS)			
polymer name:	after synthesis	after tube extrusion	after film molding	after sterilization of films
DegraPol®/btgc b8	81'000	178'000	97'000	94'000
DegraPol®/btgc b14	66'500	91'500	96'000	110'500
DegraPol®/btgc b17	61'500	105'500	77'500	89'000
DegraPol®/ btgc b41	160'500	339'000	-	-

Sterilizability. Compression-molded films were sterilized in ethylene oxide gas at 40 °C for 6 hours and left to degas for 12 hours in air. The reduction of the molar mass, taken as an indicator for the polymer stability during sterilization, was less than 10 % for all

polymers. Thus, the polymers are considered to be stable under these sterilization conditions. (Table 8)

Conclusion

It is possible to extend the family of DegraPol® polymers to members with minimal content of PHB (8 wt-%), still having crystalline PHB domains and amorphous domains containing all the soft segments and some of the PHB, by using fractionated PHB-diols as hard segments. The polymers are processable through standard processing routs of thermoplastics, show mechanical properties of reinforced rubbers, and may therefore be regarded as thermoplastic elastomers. Two different types of morphologies, one spherulithical, the other lamellar going through the entire samples, were found in the different polymers, depending on the PHB content of the block-copolymers. These morphologies may influence the final PHB structure, the degradability, and the resorbability of these polymers.

CHAPTER 3

Design Criteria for Tubular Implants

Introduction

The mechanical properties of an implant depends both on the material properties and on the geometry of the implant. To know how the implant properties can be controlled means to be able to design implants with desired properties. Even without well defined mechanical requirements, this knowledge will favor the development towards mechanically optimized implants. One possible optimization of nerve guidance channels is to make the wall thickness as thin as needed for mechanical stability. This reduces the total amount of implanted material that will have to be resorbed. It also reduces material strength during degradation and helps to break down the implant to small pieces during degradation. Smaller pieces will be faster resorbed in erosive resoption processes and in diffusion controlled resorption processes.

The nerve guidance channel is a mechanically simple implant-type. Its shape is cylindrical and the load on the implant is mainly static. As nerves are usually very sensitive to compression, the pressure from the surrounding tissue may be assumed to be rather low. Using the formulas of this chapter, the strength of the implants used can be quantified in a simple way.

Synthetic vascular grafts of small diameters represent a still unresolved medical problem. This type of implant is much more complicated, compared to the nerve guidance channel: the loadings are dynamic and the direct contact with blood represents

a completely different problem of biocompatibility. The theoretical considerations of vascular grafts in the second part of this chapter, intend to define the mechanical requirements of a such implants. If not adapted to the application, the dynamic response of the implant may cause harmful perturbations of the pulsatile blood flow.[39] A simple flow model for this type of tubular implant will also be presented. In order to limit the content of this study, no further investigations aimed at vascular grafts will be carried out here. Based on the presented relations, a mechanical optimization of vascular grafts should be straight forward for future developments.

Static Mechanical Properties

The basic laws on the strength of materials will be applied to tubular structures in the paragraphs below. The elastic modulus of the tube material is E, the radius of the tube is r, the wall thickness h, and tube length l.

Kinking

Generally, tubular implants should not kink when bended. When bended, the cross-section of a tube first becomes oval. At a certain critical bending radius ρ_{cr}, the flattening of the tube circumference becomes unstable, and the tube kinks. This critical bending radius can be estimated, comparing the energy required to bend a tube keeping the circular cross section with the energy needed to bend a tube and flatten its cross section. The resulting relationship has been published by different people in a similar form:[40,41]

$$\rho_{cr} = \lambda \cdot \frac{r^2}{h} \qquad (3.1)$$

Depending on the mechanical model applied, theoretical values of the parameter λ between 0.3 and 0.7 were given. Our experimental value, measured on a series of DegraPol® tubes with different dimensions, was 0.52.[31]

Radial Loading

A radial load P, acting over a tube of length l, will also ovalize a tubular implant. For small displacements δ in the direction of the tube radius, the implant stiffness can be estimated from the stiffness of a cylindrical shell:[42]

$$\frac{\delta}{P} = \frac{3\pi}{l} \cdot \frac{r^3}{Eh^3} \tag{3.2}$$

Bending

The bending stiffness of a straight tube can be estimated from the bending stiffness of a bar with annular cross-section fixed at one end and loaded laterally on the other end. With r_a for the outer, and r_i for the inner tube radius ($r_a = r_i + h$) the expression for that case is:[42]

$$\frac{\delta}{P} = \frac{4}{3\pi} \cdot \frac{l^3}{E \cdot (r_a^4 - r_i^4)} \tag{3.3}$$

Compliance

The compliance describes the tendency of a tubular implant to be blown up by an inner pressure. It is defined by the ratio of the relative diameter increase $\frac{\Delta r}{r}$ to the corresponding increase of internal over pressure Δp and is given by:

$$\frac{\Delta r}{r \cdot \Delta p} = \frac{r}{E \cdot h} \tag{3.4}$$

Resuming these relations, the critical bending radius of a tube for kinking does not depend on the elastic modulus of the tube material and can be reduced by increasing the wall thickness of the tube. All other presented kinds of tube stiffness depend linearly on the elastic modulus of the tube material and in some non-linear way on the geometry of the tubes.

Pulsatile Flow in a Blood Vessel Implant

The flow resistance of a pulsatile flow through a blood vessel implant is composed of two components. The frictional part can be described by the Hagen-Poiseuille-equation (equation 5) and depends on the tube size. The capacitive part depends on the tube compliance (equation 4) and is described by equation 6. On both transitions, from the blood vessel to the implant and from the implant to the blood vessel, the abrupt change of the flow resistance causes partial reflections of the pulsatile flow and a local increase of the blood pressure. The amount of this increase depends mainly on the mismatch of the implant- and blood vessel compliance.[43]

Frictional flow resistance Z_R of a laminar flow of a Newtonian fluid of viscosity ν through a tube of diameter r and length l:

$$Z_R = \frac{8\nu l}{\pi r^4} \tag{3.5}$$

The capacitive resistance Z_C of a fluid of density ρ through a tube of compliance C will be:

$$Z_C = \frac{\sqrt{\rho}}{\pi\sqrt{2}} \cdot \frac{1}{r^2\sqrt{C}} \tag{3.6}$$

The total resistanceZ_{tot} is equal to the sum of both components:

$$Z_{tot} = Z_R + Z_C \tag{3.7}$$

The reflection factor k indicates the ratio of the pressure amplitude of the incident wave p_1 to the pressure amplitude of the reflected wave p_2. k can be expressed as a function of the total flow resistance of the implant Z_{imp} and of the total flow resistance of the blood vessel Z_{bv}

$$k = \frac{p_2}{p_1} = \frac{Z_{imp} - Z_{bv}}{Z_{imp} + Z_{bv}} \tag{3.8}$$

From continuity considerations, at the blood vessel-implant transition, the sum of all

pressure amplitudes, the incident, the reflected and the transmitted (p_3) one have to be equal zero.

$$p_1 + p_2 = p_3 \tag{3.9}$$

The maximum pressure at the transition is equal p_3 which can be expressed by p_1 and the reflection factor k:

$$p_3 = (1 + k) \cdot p_1 \tag{3.10}$$

Example

Using the above mentioned relations, the influence of the wall thickness on the mechanical properties of a tube shall be estimated. The inner diameter of the tube is fixed to 1.5 mm, the tube length is 10 mm, the Young's modulus of the tube material is 10 MPa. The following estimated values are given as a function of the wall thickness in the Figures:

- Figure 12 A) shows how much the tube would be **flattened** by radial load.
- Figure 12 B) shows the **bending stiffness**, defined as the ratio of load P applied to the free tube end, to the lateral displacement d of the free tube end.
- Figure 12 C) shows the **reflection factor** k of a tube-blood-vessel transition, where the blood-vessel compliance is 5 $(MPa)^{-1}$,[44] the blood viscosity 0.005 Pa·s [45] and the blood density 1060 $kg \cdot m^{-3}$.[45]
- Figure 12 D) shows the **compliance** of the tube.
- Figure 12 E) shows the critical bending radius for **kinking**.

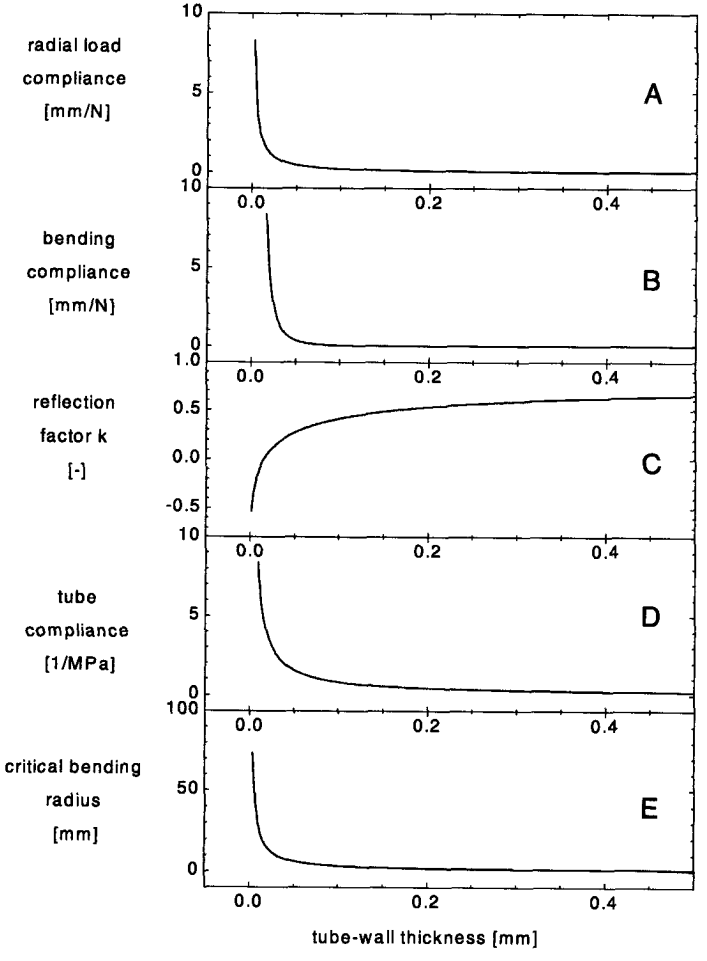

Figure 12 Estimated dependence of mechanical tube properties, when the wall thickness of a 10 mm long tube of 1.5 mm inner diameter is changed.

All tubes with a tube wall thicker than 0.1 mm (inner diameter = 1.5 mm) may be considered as stiff tubes, as the mechanical properties do no longer depend on the wall

thickness of the tubes. Figure 12 suggests that a wall thickness of about 0.05 mm would give the best combination of critical bending radius, tube stability and pulse wave reflection factor. To further improve all the mentioned properties simultaneously, the tube design would have to be altered. For a reduction of the critical bending radius, structures that increase the stiffness in the tangential direction and lower the stiffness in the longitudinal direction would have to be made. Such structures are, e.g., rippled tubes commonly used for vacuum cleaners or bendable drinking straws. The reflection factor of a pulsatile flow at the transition to a blood vessel implant may be improved by an oval tube design. Oval tubes can increase their cross-sectional area by changing their cross section from oval to round. This requires much lower forces than the stretching of the tube walls by internal pressure. Foam walled tubes could be a way to improve both, the kinking-resistance and the reflection factor. Compared to compact walled tubes they can be made more compliant with a bigger wall thickness.

Mechanical Requirements of Nerve Guidance Channels

Nerve Guidance Channels of different wall thicknesses were used. Generally, those tubes that could be handled before being implanted, had a sufficiently high mechanical strength for the application. A maximal radial compliance of about 1 mm/N could be defined from the *in vivo* experiments. A critical bending radius of about 10 mm was small enough for a successful use of the produced implants.

CHAPTER 4

Processing of the Polymers

Introduction

DegraPol®-polymers were conceived to be easy to process. Crystalline domains melting below the limiting safe processing temperature of the polymer should allow melt-processing above the melting point and give mechanical stability to the material below. A good connection between the crystalline and the amorphous domains should be achieved using multiblock copolymers where each chain potentially has some chain parts in crystalline domains as well as in amorphous domains. The building units of the polymer chains were also chosen as to make the polymer soluble in many common solvents. Both, the solubility and the melt processability of DegraPol® have been demonstrated in previous work by melt-casting DegraPol® to films and by processing DegraPol®-solutions to open porous foams.[3,5] The extrusion of DegraPol®, as described in this chapter, is a stronger test of the melt-processability. During melt-extrusion, additional parameters such as the viscosity of the melt and the solidification behavior of the polymer interfere and could prevent a successful melt-extrusion. Simultaneously this chapter describes the first small-scale production of DegraPol® implants in a semi-continuous process. It shows how tubular DegraPol® implants could be produced in a simple process with low production costs. Trying to produce tubes with special properties, foamed walled tubes were also made. Such special properties are low critical bending radius combined with high tube compliance (chapter 3), or possibly size-selective permeabilities.

Materials

Polymers

Polymers with different amounts of crystallizable blocks, and with two different kinds of non crystallizable blocks, were processed. As non crystallizable blocks, either poly[ε-caprolactone] or poly[glycolid-*co*-(ε-caprolactone)] was used. PHB-diol was used in all polymers as crystallizable blocks. The compositions and the names of the polymers are given in Table 9. In chapter 2 the polymer synthesis has been described.

Table 9 Names and compositions of the used grades of DegraPol®.

	composition [wt-%]			type of non
polymer name:	crystallizable units	non crystallizable units	diurethane units	crystallizable unit
DegraPol®/ btgc b8	8	84	8	poly[glycolide-*co*-(ε-caprolactone)]
DegraPol®/ btgc b14	14	78	8	"
DegraPol®/ btgc b17	17	75	8	"
DegraPol®/ btgc b41	41	49	10	"
DegraPol®/ btc b45	45	45	10	poly[ε-caprolactone]
DegraPol®/ btc b29	29	58	13	"

Methods

Extrusion Apparatus

A plunger extruder apparatus as shown in Figure 13 was constructed for the extrusion of 3 to 15 mL of polymer-melt to slender tubes. The polymer was melted in a heating

chamber. A plunger then pressed the polymer melt through the tube die. In the first part of the die the polymer flow was divided into three channels. This part also supported the mandrel of the die. In the second part, the three polymer channels were reunited and formed the polymer tube in the circular slit of the die. After the die, the tube was filled with nitrogen with small over-pressure. The gas pressure could be controlled through a small pipe that ended in the center of the mandrel at the exit of the tube die. Finally a pair of draw-wheels allowed the retrieval of the extruded tube at a controlled speed. In that way the draw-down ratio after the die could be controlled.

The plunger was powered by a motor, gear box, spindle set up. The plunger speed was measured using a incremental encoder and controlled by the AC output signal of an IBM-AT computer. The draw-wheel speed was controlled independently in the same way. A resistance strain gauge was used to measure the plunger force and the extruder temperature was measured and recorded at three different locations of the heating chamber. At any moment during the extrusion, the processing parameters could be adjusted in the computer program.

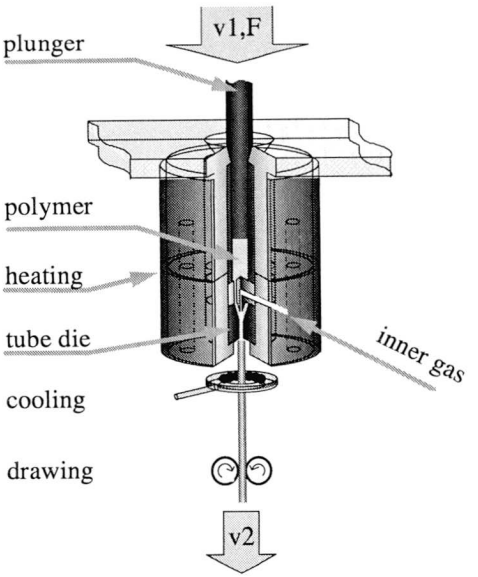

Figure 13 Drawing of the extrusion chamber of the computer-controlled plunger extruder. The extrusion chamber is set up vertically and is about 20 cm long.

Processing to Tubes

Three tube dies, with different dimensions of the circular slit, have been used for a small scale tube production (Figure 14, Table 10). The aimed inner diameter of the tubes was 1.5 mm and different wall thicknesses between 0.08 mm and 0.4 mm should have been possible. The first tube die was designed for the extrusion of relatively thick walled tubes, extruded with a draw-down ratio of about 1, and had a circular slit of 1.5 mm inner diameter and 2.3 mm outer diameter. The second and third tube dies were designed for relatively thin walled tubes, produced with a theoretical draw-down ratio of 4.84 and had an inner diameter of the circular slit of 3.3 mm and an outer diameter of 3.5 mm, respectively 3.8 mm. (Table 10). The estimated resulting tube-wall thicknesses from these dies were 0.045 mm and 0.114 mm.

Table 10 Dimensions of the circular slit of the used tube dies and total flow resistance as defined by equation 4.5.

	dimensions of circular slit		
die #	inner diameter [mm]	outer diameter [mm]	total flow resistance [$10^9/m^3$]
1	1.5	2.3	417
2	3.3	3.5	14'700
3	3.3	3.8	959

For melt extrusion, typically 5 g of polymer were fed into the preheated heating chamber. The chamber was closed with the plunger and the polymer was heated for 30 minutes. The extrusion temperature was typically chosen a few degrees higher than the melting endotherm maximum of the polymer. According to the extrusion behavior, the temperature was increased if the polymer did not form a homogeneous polymer-melt tube just after the die. If the tube could not be plastically drawn down after the die, the temperature was also increased. On the other hand, the temperature was lowered if the tube was flowing away after the die. If the measured melt pressure was higher than 200 bar, either the temperature was increased, or the extrusion speed was lowered. Typical plunger speeds were set such as the pressures in the melt were about 100 bar and depended on the die geometry. The used values were between 0.01 mm/s and 0.1 mm/s, resulting in a volumetric flow between 1.8 mm^3/s and 18 mm^3/s (Table 11). After extrusion, the tubes were hung up vertically and stored for 24 hours at room temperature.

Table 11 Typical extrusion conditions of the used dies and estimated shear rates at the die walls using equation 4.8.

die #	typical plunger speed [mm/s]	flow rate $\dot{V}$ [mm^3/s]	shear rate $\dot{\gamma}_W$ [s^{-1}]
1	0.03	0.053	0.33
2	0.01	0.018	0.99
3	0.1	0.177	1.52

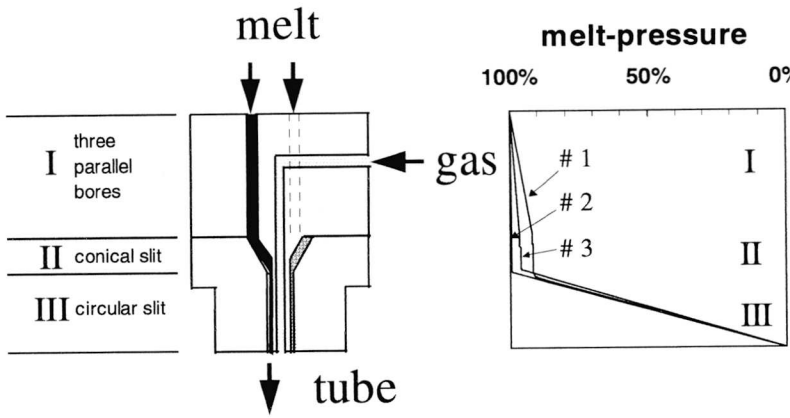

Figure 14 Section through a tube die, indicating the different sections of the dies. Polymer channels and the gas tube are shaded. Total height: 40 mm. On the right, the estimated pressure drop is given for the three sections of the tube dies.

Processing to Porous Walled Tubes

Gel Point Determination. The gel point of the used polymer solutions were determined in a rheometer (Physica, Rheolab MC100) with circular slit geometry and oscillating inner cylinder. The shear modulus of the solutions were recorded at an oscillation frequency of 1 Hz, and at a shear amplitude of 10 %. For gel point determination, solutions were cooled at 0.5 °C/min from 65 °C to 40 °C, 35 °C, and 30 °C and held at

the respective temperature for 2 hours.

Extrusion. A 15 wt-% DegraPol®/btc b29 solution in DMSO was fed into the heating chamber of the extruder at 65 °C and cooled down just below the previously determined gel point of the solution. The gel was extruded and formed a gel-walled tube. This tube was then frozen in a cool non-solvent bath, or in liquid nitrogen, after having passed an air gap of few centimeters. The frozen tubes were freeze dried and porous walled tubes were gained. The porous-walled tubes were extruded at 31 °C through an air gap of 25 mm into liquid nitrogen. A tube die with 1.5 mm inner diameter and 2.3 mm outer diameter was used. The so obtained gel-walled tubes were freeze dried at 10^{-5} bar for 18 hours.

Theoretical Evaluation of the Extrusion

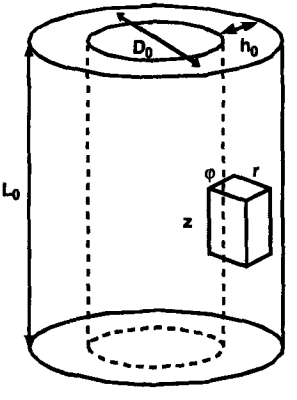

Figure 15 Tube element, indicating the annotations used in the calculation of the tube dimensions upon drawing of the tube.

Tube Geometry

The final tube dimensions depend on the geometry of the circular slit at the end of the die, on the gas over-pressure in the tube just after the die, and on the draw-down ratio after the tube die. The gas over-pressure shall be assumed to be so low as not to play any

role. Considering the polymer as an isotropic continuum, the dimensional changes of the tube, when drawn after the die, can be estimated assuming the polymer volume to be constant. Looking at a small volume ($\varphi\ r\ z$) of the tube wall (Figure 15), that is being deformed by ($d\varphi,\ dr,\ dz$), the volume conservation can be expressed in a first approximation by equation 4.1.

$$\frac{d\varphi}{\varphi} + \frac{dr}{r} + \frac{dz}{z} = 0 \tag{4.1}$$

The following definitions shall be used: Elongations along the tube axis are proportional to elongations in the z direction of a volume of the tube wall. Changes of the tube diameter are proportional to elongations in φ direction. Changes of the wall thickness are proportional to elongations in r direction. For an isotropic continuum extended in z-direction, the contraction in φ and in r direction have to be of the same amount (equation 4.2)

$$\frac{d\varphi}{\varphi} \approx \frac{dr}{r} \tag{4.2}$$

The final tube diameter D and the final wall thickness h can then be calculated knowing the draw-down ratio L/L_0, the initial diameter D_0, and the initial wall thickness h_0 (equations 4.3 and 4.4). The tube diameter and the wall thickness follow a power law of

$$\int_{L_0}^{L} \frac{1}{z} dz = -2 \cdot \int_{D_0}^{D} \frac{1}{\varphi} d\varphi = -2 \cdot \int_{h_0}^{h} \frac{1}{r} dr \tag{4.3}$$

$$\frac{h}{h_0} \approx \frac{D}{D_0} \approx \left(\frac{L_0}{L}\right)^{1/2} \tag{4.4}$$

the draw-down ratio. The exponent of both of these power laws should ideally be -0.5.

Polymer Flow in the Tube Die

As the polymer flows through the tube die, the geometry of the polymer channel changes. The pressure drop also changes with the geometry of the polymer channel. For

an incompressible Newtonian fluid of viscosity η, the pressure drop Δp can be written in the following general form:[46]

$$\Delta p = W\eta\dot{V} \tag{4.5}$$

where $\dot{V}$ is the volumetric flow rate and W the so called resistance. For a circular pipe with radius R and length L, as the three fead bores in the first part of the die, the resistance is given by equation 4.6. For a circular slit with width h, as in the final part of the die, it is given by equation 4.7. [46]

$$W = \frac{8L}{\pi R^4} \tag{4.6}$$

$$W = \frac{6L}{\pi R h^3} \tag{4.7}$$

The intermediate part, the conical slit, may be considered as a succession of circular slits with gradually changing radius and width.

The shear rates in the tube die may orient the polymer molecules and lead to a die-swell. The shear rates are the biggest at the die walls in the final circular slit of the used dies. They may be estimated by equation 4.8: [46]

$$\dot{\gamma}_W = \frac{6\dot{V}}{\pi D h^2} \tag{4.8}$$

Using equations 4.6 and 4.7, the pressure profiles in the tube dies can be estimated. They are given in Figure 14 for the used tube dies. By far the biggest pressure drop occurs in the circular slit of all tube dies. This is one of the requirements for a good tube formation, as the polymer tubes are formed there. The estimated total flow resistance of each used die, as well as the shear rates on the die walls of the circular slit are given in Table 10 and Table 11.

Results and Discussion

Plunger Extruder

The plunger extruder design allowed the dead volume of the extruder to be reduced to about 0.5 mL, thus increasing the yield of the tube extrusion. As an other possible advantage, the polymer melt was not subjected to high shear stresses when pushed by the plunger. On the other hand, the polymer melt was not additionally homogenized when melted, the process was not continuous, and the residence time of the polymer in the extruder differed between the different parts of a tube. No insufficient homogenization, nor any negative effect due to the different residence times could be observed during tube extrusion.

Melting and Extrusion Temperatures

The thermograms of the five extruded polymers are given in Figure 16. As a first attempt, the extrusion temperatures were chosen few degrees higher than the highest melting endotherm maximum of the respective polymers. The final extrusion temperatures were then adapted empirically to the extrusion behavior and are given in Table 12.

Table 12 Extrusion temperatures of the used polymers.

polymer name:	extrusion temperature [°C]
DegraPol®/btgc b8	132
DegraPol®/btgc b14	132
DegraPol®/btgc b17	133
DegraPol®/btgc b41	148
DegraPol®/btc b45	137

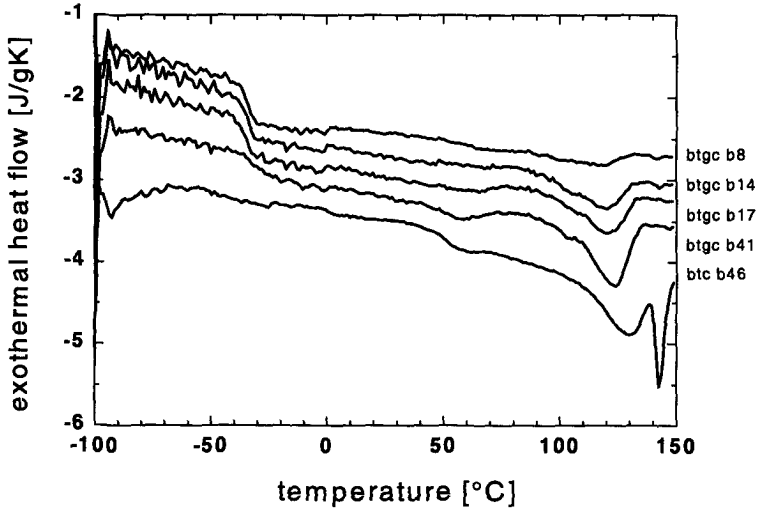

Figure 16 Thermograms of the melt extruded polymers showing a glass transition temperature around -30 °C and one or two melting signals between 110 °C and 150 °C.

Dimensions-Control

The power law between the draw down ratio and the tube diameter or the wall thickness (equation 4.4), could be confirmed in a series of preliminary experiments. A DegraPol®/ btc b46-polymer was extruded at 137 °C through the tube die with 1.5 mm inner and 2.3 mm outer diameter. The speed of the draw wheels was varied at constant extrusion velocities. Knowing the plunger velocity of 0.03 mm/s, the tube velocity when coming out of the die was estimated from the extruder geometry to be 2.2 mm/s. The draw wheel speeds were chosen between 2.3 mm/s and 12.8 mm/s, giving draw down ratios between 1.04 and 5.8. The tube dimensions were then determined on cross sections of the resulting tubes under a light microscope and are represented in Figure 17. Both exponents of the found power laws for the tube diameter (-0.45) and for the wall thickness (-0.53) are close to the theoretical value of -0.5 for uniaxialy extended tubes. The sum of the exponents is -0.98, very close to -1, the value required for volume conservation. The wall thickness is decreasing more rapidly than the tube diameter, when

the tube is drawn down after the die. This may be due to a small blowing-up effect of the inner gas pressure.

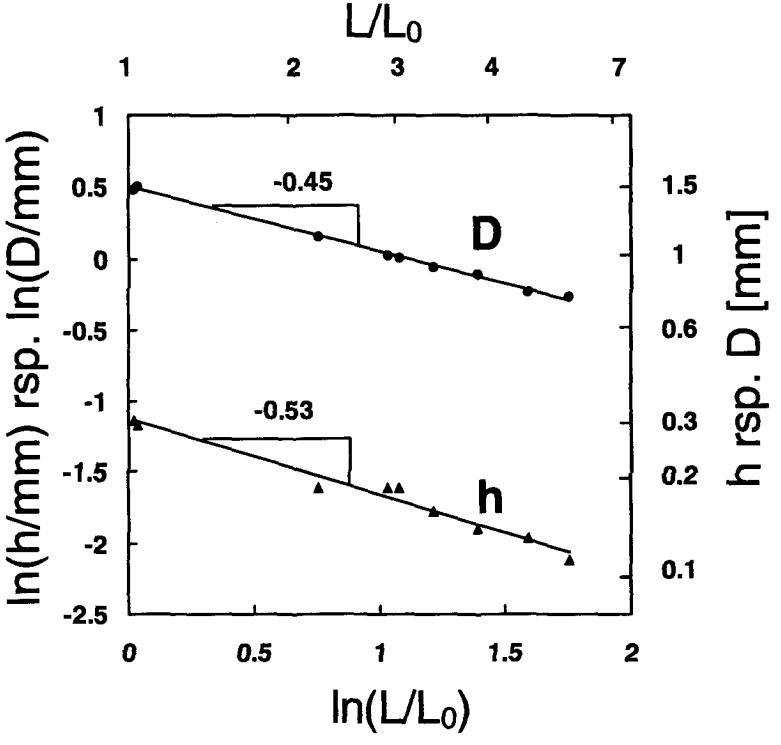

Figure 17 Changes of the tube diameter D and of the wall thickness h upon extension of the tube after the tube die.

However, none of the extruded DegraPol®-polymers allowed a stable blowing up of the tube after the die. As a consequence, the over-pressure in the tube had to be so low that it had just minor influence on the tube dimensions. The susceptibility of the tubes to be blown up by the inner gas pressure increases if the diameter of the tube is increased or if the wall thickness is reduced. One advantage of drawing the tubes after the die, was that they were straightened out in that way. Another was, that the tube dimensions could be

better controlled at higher draw-down ratios. There, the tube dimensions were less dependent on changes of the draw-down ratio, as predicted by the power law of equation 4.4.

Tube Production

Straight, smooth walled, and transparent tubes could be extruded to be used as Nerve Guidance Channels and are shown in Figure 18. The aimed wall thicknesses were 0.08 mm and 0.15 mm with an inner diameter of 1.5 mm. Due to the small wall thicknesses and to the flow behavior of the polymer melt, the tube dimensions were very sensitive to small changes of the gas pressure in the tube after the die. By controlling and adapting the extrusion parameters during the tube extrusion, tubes a few dozens of centimeters long could be obtained with an inner diameter between 1.4 mm and 2.0 mm. The desired 10 mm long Nerve Guidance Channels with 1.5 mm inner diameter were then cut from these tube pieces.

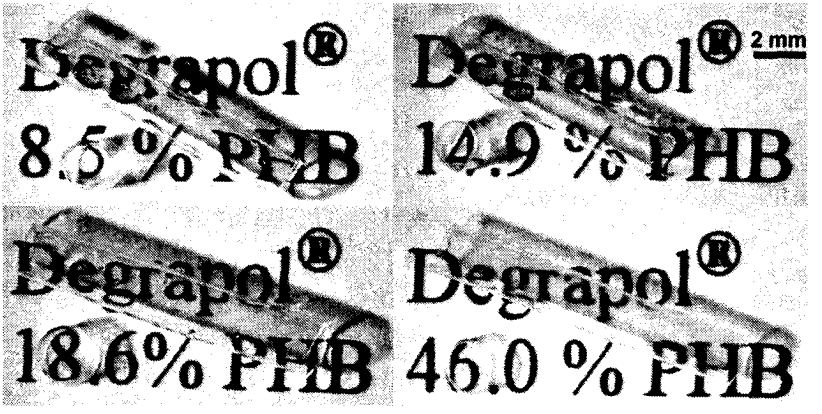

Figure 18 Photographs of extruded tubes. There is always one tube viewed from the side lying diagonally in the picture, and one viewed from the front. The indicated contents of PHB correspond to the compositions upon synthesis and may be slightly different from the polymer compositions determined by ^{1}H-NMR.

During the first hours after extrusion, the tubes were tacky and tended to stick together not being separable any more. Therefore, the tubes were hung up vertically for one day. During this time, most probably the separation into amorphous and crystalline domains progressed in the tube material, making the material less tacky. The crystallinity in the tubes was investigated by wide angle x-ray diffraction. Diffraction patterns were measured with two tube orientation, first with the tub axis in the plane of the incident and of the reflected x-ray beam (azimuthal) and second with the tube axis perpendicular to that plane (equatorial). All diffraction patterns showed the typical diffraction signals of crystalline PHB at diffraction angles of 7.6 and of 13.2. They had no major differences if the tubes were placed in azimuthal or in equatorial position. Therefore no signs of a preferred orientation of the crystalline planes in the tubes were obtained (Figure 19).

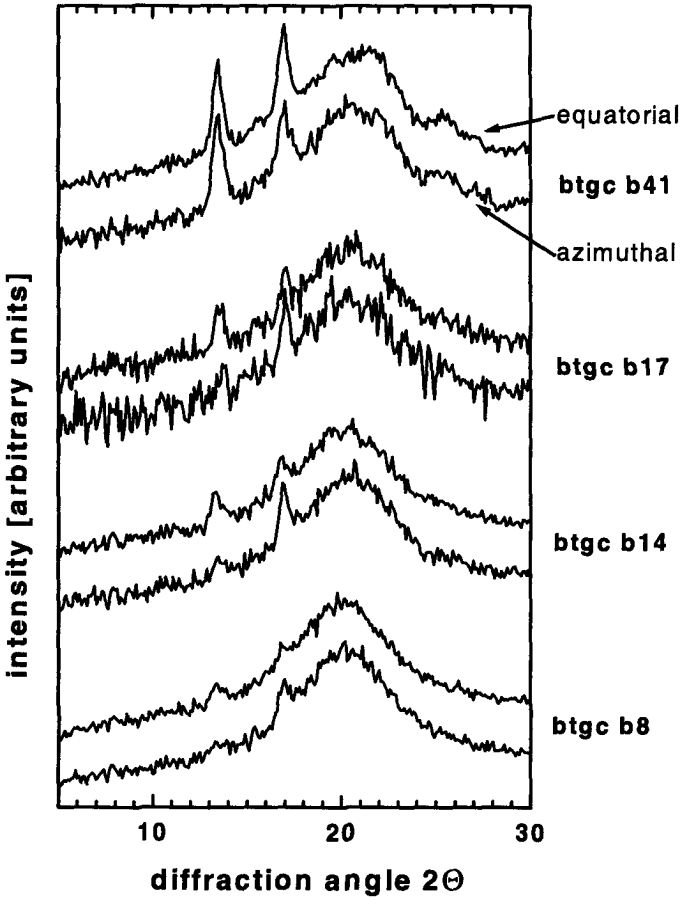

Figure 19 X-ray diffraction patterns of extruded tubes. All diffraction patterns have been taken with two different tube orientations and represent reflections from crystal planes with plane normals perpendicular to the tube axis (equatorial), and parallel to the tube axis (azimuthal).

The lack of orientation in the tubes is probably due to the low shear rates in the tube die (Table 11) and to the relatively low viscosity of the polymer melt. No die swell was observable, which also indicates a low degree of orientation in the die. The crystallization of the polymer takes place only slowly after the extrusion process, as can

be suspected by the slow diminution of the tacky behavior of the tubes in the hours after the extrusion. This should not induce any new orientation into the polymer tubes.

Foams

The solution-freezing method to produce open-porous DegraPol® foams could successfully be applied to the DegraPol®-grades with low contents of PHB. Three dimensional structures were obtained from the polymers DegraPol®/btgc b8, DegraPol®/ btgc b14, and DegraPol®/btgc b17 (Figure 20). The foams were relatively soft and compliant. Just the foams from DegraPol®/btgc b8, the polymer with the lowest content of PHB, were tacky and tended to stick to other materials as well as to itself. The foam morphology, as revealed in sections through the foams, showed a pore size of about 0.1 mm for all three types of foams. The pores had no preferred orientation and some connections between pores were visible. To serve as cell carriers for tissue engineering, the pore size would probably have to be increased. As shown in the earlier developments of DegraPol®-foams, this can be done by changing the thermal history upon freezing the polymer solution.[5]

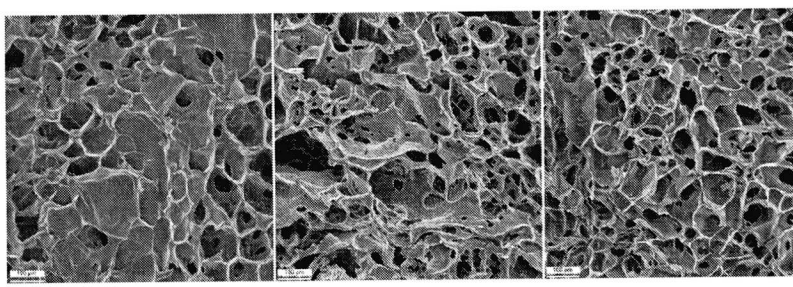

Figure 20 Scanning electron images of the solution-processed foams. On the left a DegraPol®/btgc b8-foam, in the middle a DegraPol®/btgc b14 foam, and on the right a DegraPol®/btgc b17 foam. The scale bars are 100 µm long.

Porous Walled Tubes

When cooled from 65 °C to 30 °C, 35 °C, and 40 °C, the gel formation could be observed by an increase of the shear modulus of the polymer solution. Of the tested temperatures, the increase was the fastest and the high at 30 °C. After 1 hour at 30 °C the

gel had a shear modulus of about 1000 Pa, compared to about 500 Pa at 35 °C and about 100 Pa at 40 °C (Figure 21). A shear modulus of about 1000 Pa (30 °C) has proven to give good extrusion properties. At lower shear moduli the gel walled tubes had insufficient stability after the tube die, and the tubes flew apart.

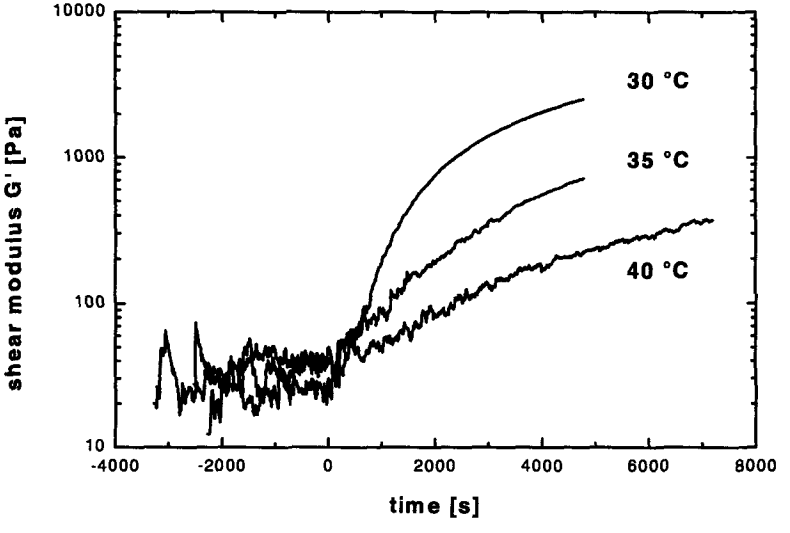

Figure 21 Shear modulus of 15 wt-% polymer solutions in DMSO, cooled from 65 °C to the indicated temperatures (negative times), and held at the indicated temperatures (positive times). The gelation of the solutions is a process that lasts for hours at the respective temperatures.

Different methods have been tried to freeze the gel-walled tubes just after the tube die and to remove the solvent from the gel walled tubes. The resulting tubes differed in their macroscopic homogeneity and in the porous structure of the wall. The best results were obtained by extruding the gels at 31 °C, through an air gap of 25 mm into liquid nitrogen and by freeze drying the so obtained gel walled tubes. These tubes had few macroscopic defects like holes through the entire tube wall. The pores in the tube walls had a narrow size distribution with an average size of about 3 μm (Figure 22). The tubes were easy to

handle, flexible and not brittle. This was also revealed by the elongations at break of 250 % to 400 % upon tensile testing of these tubes. A possible size selective permeability was indicated by the almost complete permeation of Dextrane 6'000, and the non measurable permeation of Dextrane 70'000 after 5 days.

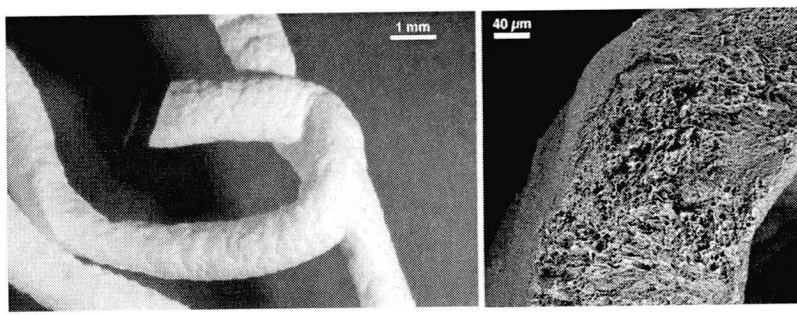

Figure 22 Left: Picture of a porous walled tube, that is white due to the light scattering at the polymer/air interfaces of the pores. Right: scanning electron microscope image of the porous structure of the tube wall. The tube axis would be in the lower right corner of the image and just a sector of the tube wall is shown.

It appeared to be possible to process DegraPol® into porous walled tubes. These tubes may have interesting mechanical properties such as being compliant and soft with a low tendency to kink. The selective permeability may be used for membrane applications and the porous structure may be loaded with biologically active substances.

Conclusion

The presented work demonstrates the processability of DegraPol®-polymers through the melt, even at low contents of crystallizable blocks (8 wt-%). Extruded at few millimeters of tube per second, the tubes had to be stored about 1 day at room temperature to reduce their tacky surface behavior. This may cause some special requirements in large scale DegraPol®-tube production. The constructed computer-controlled plunger extruder has been found to be best suited for the extrusion of small, development scale volumes of

polymer in a controlled way. Previously developed methods to obtain porous DegraPol®-structures could be applied to the more recently developed DegraPol®-polymers with low contents of crystallizable blocks. These results show, that DegraPol®-polymers can be processed through standard processing routes of thermoplastics. Their processability through the melt and through solutions offer a great liberty in designing medical implants.

CHAPTER 5

Degradation in Buffer Solutions

Introduction

Used as a biomaterial, DegraPol® may degrade by different processes. One of them is the pure hydrolytic degradation without any influence of enzymes or cells. This kind of degradation can be simulated by storing DegraPol® in buffered water solution at constant temperature. A degradation profile of each DegraPol®-grade can be determined by measuring physical and chemical properties, such as molar mass, crystallinity, or chemical composition, after different periods of time. Comparing the degradation profile from hydrolytic degradation in buffered water solutions with the degradation profiles of implanted material, the influence of hydrolytic degradation upon implantation may be estimated.

Results

Hydrolytic Degradation

Within the first 5 weeks of hydrolytic degradation, the molecular weight of the copolymers was drastically reduced to values of a few thousand. Neither the monomer unit composition nor the crystallinity in the polymers did change considerably, as shown by the NMR spectra and the X-ray diffraction patterns (see Table 13). During the following weeks of degradation, the glycolate-unit content was observed to decrease. The decrease in ε-caproate units was less distinct but still significant. In this second

period of degradation, the physical changes of the polymers were quite noticeable. Being tough and elastomeric at the beginning, the polymer containing 41 wt-% of PHB units became hard and very brittle. The three polymers with 17, 14, and 8 wt-% PHB units became waxy, almost liquid, and very tacky in that period of degradation. The 8wt-% PHB copolymer-tubes lost almost all of their mechanical stability. They were kept in their tubular shape probably only due to the capillary pressure of the buffered water. When the water was removed from the lumen of these tubes, they collapsed, becoming completely flat polymer strips. All the polymers acquired significant opacity during hydrolytic degradation. In the polymer containing 41 wt-% of PHB, this was most probably due to the high number of interspherulithical cracks of about 1 μm opening width, spread over the entire samples (Figure 23). In the case of the three polymers with lower PHB contents, the opacity can not be explained so readily. Interestingly, the opacity almost completely disappears upon drying of these three types of polymers.

In Figure 24, the inverse molecular weight is displayed as a function of time, revealing the molar mass changes towards the end of degradation. Interestingly, the degradation rates of all polymers investigated were comparable and did not depend on the content of the faster degrading soft segment. Obviously, other factors than the chemical composition of the copolymers, possibly the polymer morphology or the permeability towards small molecules, also have a great effect on the degradation rate.

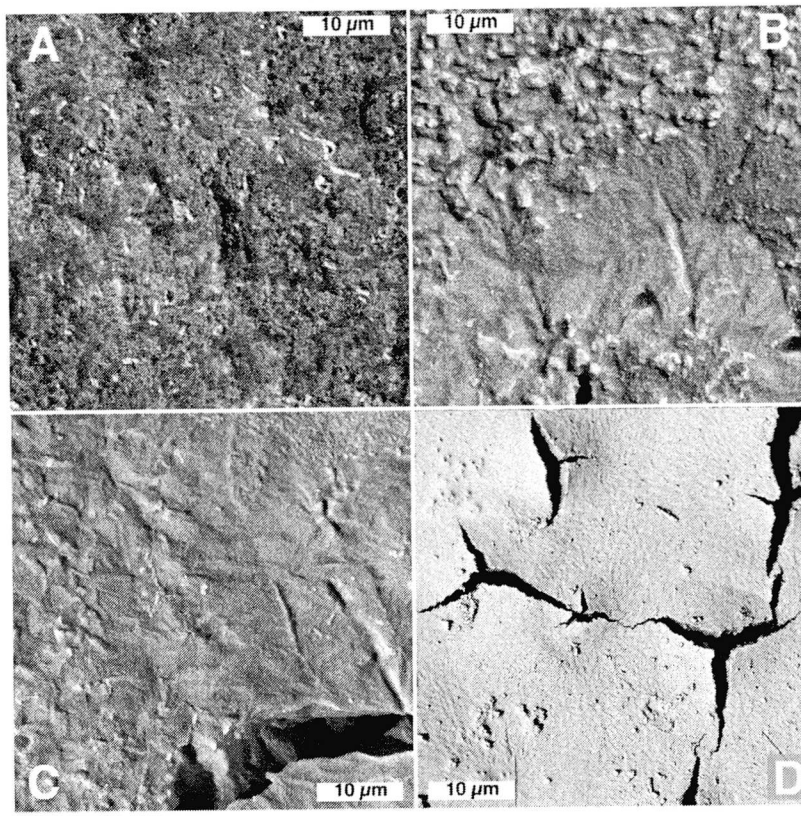

Figure 23 Scanning micrographs of polymer films degraded in buffered water solution (pH 7, 37 °C). A: DegraPol®/btgc b8, B: DegraPol®/btgc b14, C: DegraPol®/btgc b17, D: DegraPol®/btgc b41.

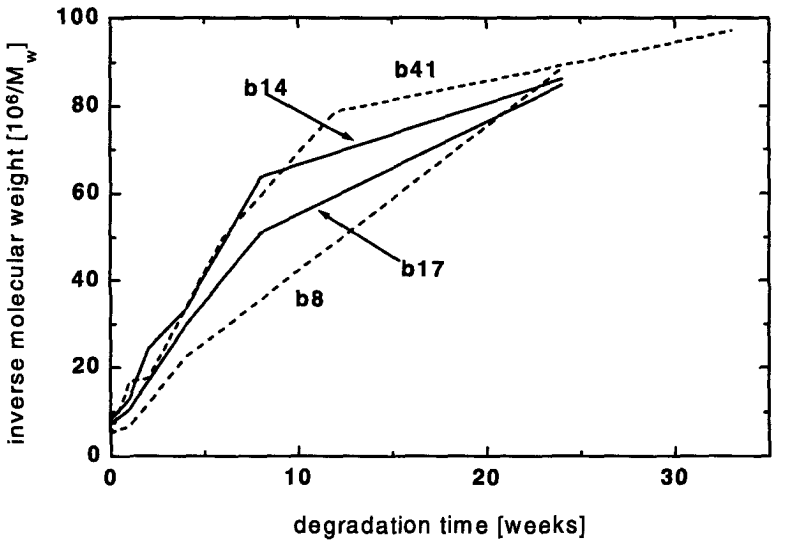

Figure 24 Inverse molecular weight, measured by means of GPC, as a function of the degradation time in buffered water solution. (DegraPol®/btgc b8, DegraPol®/btgc b14, DegraPol®/btgc b17, DegraPol®/btgc b41)

Table 13 Chemical composition of the polymers after different times of degradation in buffered water solution (pH=7, 37 °C).

polymer name:	degradation time [weeks]	composition [wt-%] hydroxy butyrate/ valerate units	hydroxy caproate units	glycolate units	diurethane units	ethylene glycol units
DegraPol® /btgc b8	1	9	56	26	7	2
	2	10	56	26	7	2
	15	10	58	23	7	2
	24	11	58	22	6	2
DegraPol® /btgc b14	1	14	53	24	7	2
	2	15	53	24	7	2
	15	16	54	21	8	2
	24	17	56	19	6	2
DegraPol® /btgc b17	1	18	51	23	7	2
	2	18	51	23	7	2
	15	16	55	21	5	2
	24	21	53	19	5	2
DegraPol® /btgc b41	2	41	35	14	9	1
	12	48	33	9	9	1
	15	53	29	8	10	1
	33	65	19	4	11	1

Conclusion

These polymers have similar hydrolytic degradation characteristics as the corresponding polymers with higher PHB contents, but the remaining amount of PHB after degradation is lower. The polymers with low PHB contents become waxy, tacky, and almost liquid upon degradation, and do not become as brittle as the polymers containing 41 wt-% PHB.

CHAPTER 6

Cell Compatibility

Introduction

Previous grades of DegraPol® were extensively tested for cell compatibility in cell culture tests.[2,3,5,9] In general, the cell compatibility was comparable to the compatibility of standard polystyrene tissue-culture plates. Some of the faster degrading DegraPol®-grades were first degraded in cell culture medium for time periods up to 50 days before the cell compatibility was tested.[29] Degrading the polymers before the cell compatibility testing did not affect the test results.

A set of cell culture tests was selected to situate the compatibility of the newer grades within the compatibility of the already tested DegraPol®-grades. As the polymers were fast degrading, cell culture tests were also performed on samples degraded up to 56 days before the tests.

Results

Cell Compatibility

No morphological difference was observed either in macrophages (macrophage cell line J774), in fibroblasts (fibroblast cell line 3T3), or in osteoblasts (osteoblast cell line MC3T3) cultured on melt cast films of DegraPol®/btgc b8, DegraPol®/btgc b14, or DegraPol®/btgc b17. The morphological integrity was maintained on all polymers after degradation intervals of 0, 4, and 8 weeks. Compared to cells cultured on tissue culture

polystyrene (TCPS), cells exhibited reduced levels of cell density on not pre-degraded polymer films (35-60 % of TCPS). DegraPol®/btgc b8 and DegraPol®/btgc b14 films pre-degraded for 8 weeks, showed a significant increase in the cell density of fibroblasts and osteoblasts but not of macrophages. After 8 weeks of pre-incubation, osteoblast showed remarkably higher cell density compared to TCPS (180 % of TCPS).

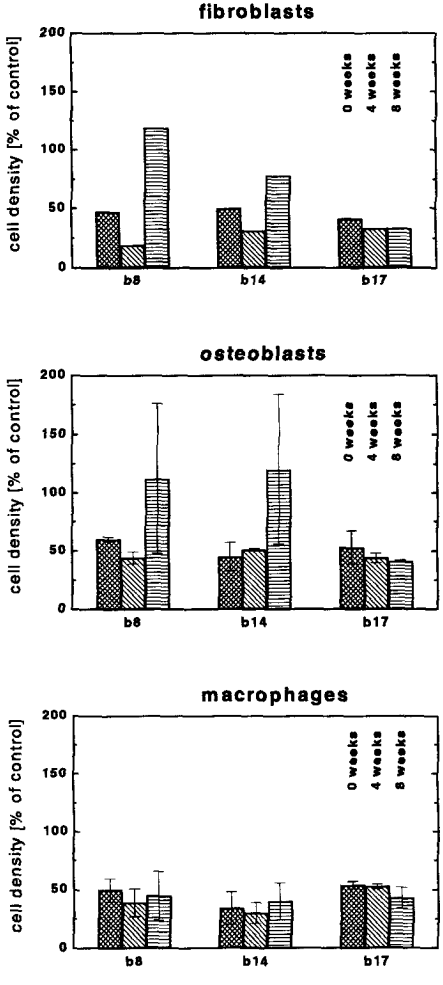

Figure 25 Cell density of fibroblasts, osteoblasts, and macrophages cultured on DegraPol®/btgc **b8**, DegraPol®/btgc **b14** and DegraPol®/btgc **b17**, pre-degraded for 0, 4, and 8 weeks. Cells cultured on tissue culture polystyrene are taken as controls. All represented tests were carried out on three samples. The results given for macrophages and osteoblasts are average values of two experiments, the error bar indicating the two measured values.

The production of nitric oxide (NO), a marker for activated macrophages, was elevated in macrophages cultured on the test polymers. NO-levels were further increased with increased incubation time. The increase in NO-production may be due to phagocytosis of DegraPol degradation products as already described.[9]

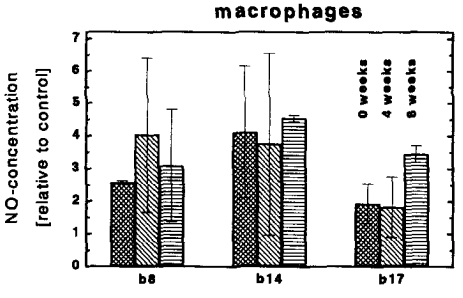

Figure 26 Nitric oxide (NO) levels in the supernatant of macrophages cultured on polymers (DegraPol®/btgc **b8**, DegraPol®/btgc **b14** and DegraPol®/btgc **b17**, pre-degraded for 0, 4, and 8 weeks). The determined NO levels are divided by the NO levels of the control cultures and by the macrophage density determined by the MTT test. The represented values are averages of two experiments, each carried out on three samples. The error bars indicate the values mesured in the two tests.

Conclusion

The level of macrophage-, fibroblast-, and osteoblast-survival on DegraPol®-grades developed here for nerve guidance channels was as good as on the previous grades of DegraPol®. Macrophages were not excessively activated on the surface of these grades of DegraPol®. In their initial state, the tested cells revealed no major difference of cell-compatibility between the three tested polymers. The survival of fibroblasts and of osteoblasts seems to be sensitive to the degradation of the polymer films before cell-testing. After four weeks of pre-degradation the survival of these cells on DegraPol®/ btgc b14 and on DegraPol®/b8 has been reduced. This may be the effect of higher concentrations of cytotoxic degradation products. After 8 weeks of pre-degradation, the survival has increased to the highest measured values for these polymers. This could be

due to a remaining cell-compatible structure after the first steps of polymer degradation. These highly suggestive interpretations are supported by the fact, that the described effects are more pronounced on the DegraPol®-grade with the highest degradation rate.

CHAPTER 7

Performance as Nerve Guidance Channels

Introduction

The golden standard of clinical nerve repair procedures consists in the coaptation of both severed nerve endings using fine suture material or by interposing an autologous nerve graft between severed nerve ends in the case of larger nerve defects. Nerve guidance channels (NGCs) are polymeric tubular conduits onto which both severed nerve endings can be sutured. They offer a potential alternative to autograft repair of large nerve defects. In a recent study, collagen-based NGCs were compared to autologous nerve grafts or direct suture repair in a transected median nerve primate model.[15] After 3.5 years no significant difference in behavior, electrophysiology and morphological appearance between each repair technique could be detected.

Besides simplifying suturing procedures and preventing scar tissue ingrowth into the regenerating environment, NGCs can be designed to positively effect the regenerating process. NGCs releasing trophic factors or containing artificial extracellular matrix-like material within their lumen have been reported to enhance peripheral nerve regeneration.[16,17,18] However, upon completion of regeneration the channel structure no longer serves any purpose. In fact, it may become detrimental due to mechanical impingement or infection.[19] Besides making secondary surgery unnecessary, biodegradable NGCs potentially avoid these problems. Different biodegradable materials have been tested experimentally, such as polyglycolic acid, amorphous copolymers out of D,L-lactic acid and ε-caprolactone and polyurethane-based

materials.[20,21,22,23,24,25,26] NGCs have also been fabricated out of biological polymers such as collagen or hyaluronic acid.[27,28] All these polymer systems were accompanied by swelling of the tube's wall which may potentially impede the nerve regeneration process by occluding the channel's lumen. Also, degradation rates were rather slow as the integrity of the channel structure was still preserved after 3 months.[24] The biosafety issue related to animal derived material such as prions from bovine derived collagen and difficulties in predicting resorption rates also justifies the further investigation of substitute synthetic material for nerve guidance channels.

In this study, the newly synthesized DegraPol®-grades (chapter 2) were evaluated. They represent a set of polymers, differing in the content of crystallizable blocks. As described in chapter 4 they were processed into NGCs. The material and implant properties were adjusted to match the desired degradation rates and the required mechanical properties of the NGCs for a transected rat sciatic nerve model. The implant behavior and the nerve regeneration process was analyzed at 4, 12 and 24 weeks post-implantation.

Materials and Methods

The polymers used were synthesized as described in chapter 2. They are phase-segregated multiblock copolymer prepared by co-condensation of telechelic, low molar mass poly[(*R*)-3-hydroxybutyric acid-*co*-(*R*)-3-hydroxyvaleric acid]-diol (PHB, forming crystalline domains) and poly[glycolide-*co*-(ε-caprolactone)]-diol (present in amorphous domains), coupled with aliphatic, 2,2,4-trimethylhexamethylen diisocyanate (TMDI) as chain extender. Table 14 displays the composition and some physical properties of the polymers used. The values for the Young's modulus varied between 1.9 and 46 MPa at day 0. Polymers with the lowest values exhibited tissue-like properties at the time of

implantation.

Table 14 Composition and properties of the used DegraPol®/btgc-polymers.

polymer name:	crystallizable blocks (PHB) [wt-%]	non crystallizable blocks [wt-%]	junction units (TMDI) [wt-%]	Young's modulus [MPa]	T_g [°C]	T_m [°C]	M_w
DegraPol®/ btgc b8	8	84	8	1.9	-35	122	178'000
DegraPol®/ btgc b17	17	75	8	8.4	-35	120	105'000
DegraPol®/ btgc b41	41	49	10	46	-30	123	160'000

In vivo Assay

Nerve Guidance Channel Preparation. NGC with 1.5 mm inner diameter were melt extruded with a mean wall-thickness of 138 ± 47 mm, using a laboratory made, computer controlled plunger extruder, specially designed for the extrusion of small quantities of thermoplastic polymers into slender tubes. The final tube dimensions were obtained by careful control of the gas pressure in the lumen of the tubes and of the longitudinal extension of the tube after extrusion from the die. All channels were cut to 10 mm length.

Implant Sterilization. The NGCs were gas sterilized using ethylene oxide at 30 °C. Prior to implantation, guidance channels were allowed to degas for at least two days.

Implantation Procedure. The right sciatic nerve of a pentobarbital-anesthetized (50 mg/kg) male Wistar rat was exposed through a skin incision along the anterior medial aspect of the thigh after retracting the gluteus maximus muscle. The sciatic nerve was mobilized from the ischias tuberosity to the tibial-peroneral bifurcation by gentle dissecting the overlying connective tissue sheets. The proximal and distal nerve stumps of the transected nerve were secured within the 10 mm long guidance channel lumen with a single 10-0 nylon suture. Both nerve ends were positioned 1 mm from the channel

ends, so that the proximal and distal nerve stumps were separated by an 8 mm gap. The channel was then filled with sterile saline using a 25G seringe. The surgical site was irrigated with sterile saline. Muscle approximation and skin closure was achieved with a 6-0 polylactic acid and a 4-0 monofilament nylon suture respectively. Aseptic surgical techniques were maintained throughout the procedure, which was performed under a Zeiss operating microscope. A total number of 26 animals were implanted (Table 15). Cohorts of animals were implanted with 41 wt-%, 17 wt-% or 8 wt-% PHB containing nerve guidance channels. Animals were caged in pairs and housed in a controlled environment with 12 hour on-off light cycles. Food and water was provided ad libitum.

Table 15 Number of animals and implantation time in each experimental group; n.d.: not done.

polymer name:	4 weeks	12 weeks	24 weeks
DegraPol®/btgc b8	4	4	2
DegraPol®/btgc b17	2	n.d.	2
DegraPol®/btgc b41	4	4	4

Implant Retrieval and Evaluation. Upon termination of the experiments, the animals were deeply anesthetized with pentobarbital. The operative site was reopened and the channel was prepared for visual inspection. Photographs were taken with a camera mounted onto the surgical microscope. Afterwards, guidance channels were removed together with 3 mm of native nerve at either end. The explant was immersed in 4 % paraformaldehyde and 2.5 % glutaraldehyde in PBS at pH 7.4 and fixed for at least 3 days. For histological analysis, channels were post-fixed in a 1 % osmium tetroxid solution, dehydrated and embedded in Epon (Fluka, Switzerland). Transverse sections of 1 mm thickness were cut on a Leica 2065 microtome. Semithin sections for light microscopy were stained with toluidine blue. The number of myelinated axons, density of myelinated axons and the cross-sectional area of the regenerated nerve cable at the channel midpoint were investigated. Polymer degradation was studied at 4, 12 and 24 weeks. Channel segments designated for polymer analysis were separated from surrounding tissue, rinsed in water and dried in vacuo, without fixation.

Results

Macroscopical and Histological Evaluation

Tissue Reaction to Implant of DegraPol®/btgc b8. After four weeks of implantation, a large crack had formed along the longitudinal axis of all channels. The remaining part of the NGC had contracted around the regenerated tissue cable like a sleeve. Loosing its transparency, the polymer conduit altered its mechanical properties changing from a rubber into a wax-like material (Figure 27 A). A thin loosely attached connective tissue capsule developed around the guidance channel. It was composed of several layers of interlaced fibroblasts (Figure 28). At 12 weeks, several long cracks became apparent on the channel surface. The channels had fractured into 2 to 3 pieces. Numerous macroscopical blood vessels covered the channel structure penetrating the channel lumen through the cracks at different locations (Figure 27 B). Upon histological examination, a connective tissue capsule engulfing the guidance channel material was observed. At 24 weeks, it became difficult to discern the channel material containing the regenerated tissue from the original nerve proximal and distal to the site of the lesion (Figure 27 C). The macroscopical tissue reaction around the channel was minimal. Upon histological examination, it became apparent that the channel remnants had collapsed onto the regenerated neural tissue. The remaining material consisted of polymer fragments that were held together by layers of connective tissue separating them from each other (Figure 29 A). Inflammatory cells composed mainly of macrophages and giant cells covered the surface of small individual fragments (Figure 29 B, C).

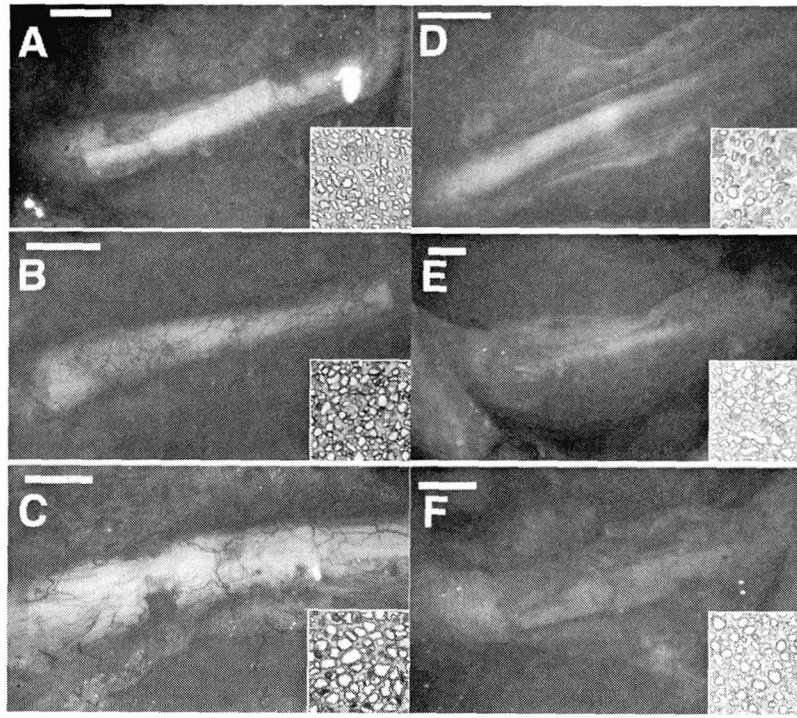

Figure 27 Macroscopical appearance of the implant site. Micrographs A, B and C display NGCs with 8 wt-% PHB at 4, 12 and 24 weeks. Micrographs D, E and F show NGCs with 41 wt-% PHB after 4, 12 and 24 weeks. Inserted micrographs show myelinated axons at the channel midpoint (50 μm x 50 μm). Scale bar ≈ 0.2 mm.

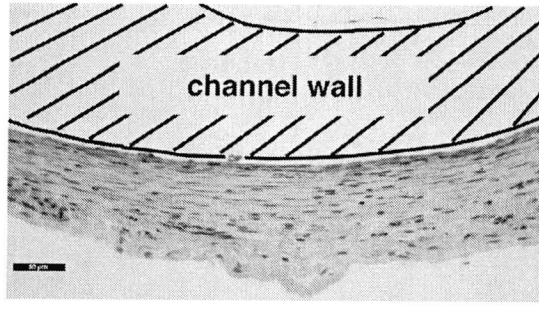

Figure 28 Photomicrograph displaying the tissue capsule on the exterior aspect of the NGC after 4 weeks. Part of the NGC wall is represented schematically. Scale bar = 50 μm.

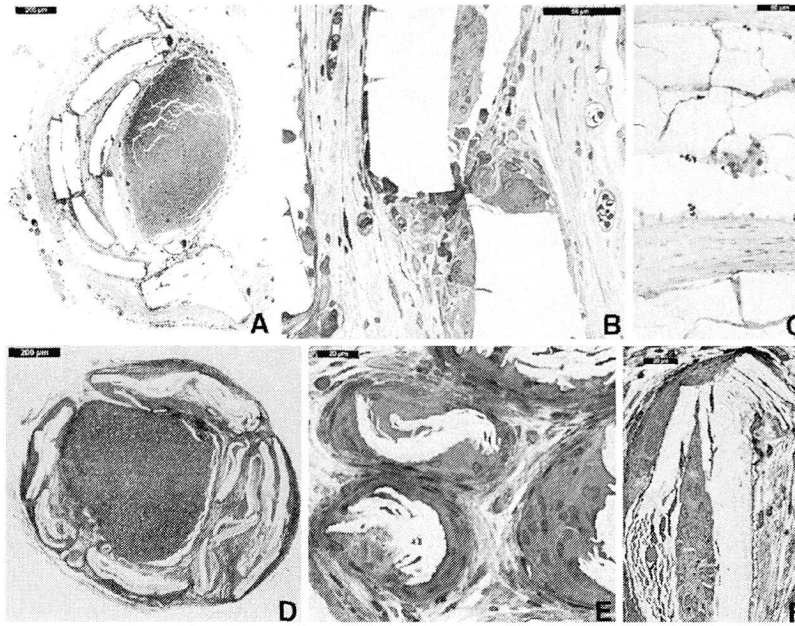

Figure 29 Microscopical appearance of DegraPol®/btgc b8 (A, B, C) DegraPol®/ btgc b41 (D, E, F) after 24 weeks. Images A and D show the regenerated nerve cable within connective tissue surrounded by polymer fragments. Images B, C, E and F display the inflammatory reaction occurring at the surface of individual polymer pieces including macrophages and giant cells.

Tissue Reaction to Implant of DegraPol®/btgc b17 and b41. The time course of degradation of both polymers was significantly slower compared to DegraPol®/btgc b8. After 4 weeks of implantation, the overall structure of the guidance channels was still intact. Polymers had remained transparent and had kept their elastic properties (Figure 27 D). Gentle manipulation by surgical forceps inflicted no mechanical damage to NGCs. A connective tissue capsule had formed around the exterior of the nerve guidance channel. After 12 weeks of implantation, large cracks became visible at the open ends of the channels and along the longitudinal axis (Figure 27 E). Microcracks were also observed under the surgical microscope throughout the channel structure. The polymer

had turned from an elastic into a brittle material. Upon gentle manipulation with surgical forceps, NGCs fractured into several large pieces. Granulation tissue had infiltrated the interior of the lumen through the formed cracks and surrounded the regenerated nerve cable.

After 24 weeks, the polymer channel had fragmented into several pieces (Figure 27 F). The channel fragments were grouped around the regenerated nerve cable and were held together by layers of connective tissue. The size of individual fragments was larger and the morphology of the polymer pieces more regular as compared to DegraPol®/btgc b8 channels (Figure 29 D, E). Numerous macrophages intermingled with sparse giant cells were observed on the surface of individual channel remnants trying to engulf smaller polymer particles (Figure 29 F).

Nerve Regeneration in DegraPol®/btgc b8. Eight out of 10 implanted NGCs contained a regenerated nerve cable. In two animals, the interior of the channel was devoid of any regenerated tissue. In the remaining eight animals regenerated tissue cables had formed in the lumen of NGCs after 4 weeks, despite granulation tissue ingrowth through channel wall cracks. These cables were centrally located and free from any tissue adhesion to the channel wall. They were composed of an epineurial tissue surrounding myelinated axons and Schwann cells grouped in small fascicles. Increasing numbers of myelinated axons were detected over time (4 weeks: 3908 ± 436; 12 weeks: 6967 ± 806). At 12 weeks the axonal density had remained constant, while the mean cable area had increased. A relatively thick epineurial tissue sheath composed of several layers of interdigitating fibroblasts surrounded the regenerated tissue. After 24 weeks, axonal counts, axonal density as well as the nerve cable area had remained stable (5891 ± 381) as compared to 12 weeks (Table 16). The inflammatory reaction occuring on the surface of polymer fragments was well separated from the regenerated neural tissue and did not seem to effect it.

Nerve Regeneration in DegraPol®/btgc b17 and b41. Fifteen out of 16 implanted NGCs contained a regenerated nerve cable composed of numerous myelinated axons and

their Schwann cells encased within small fascicles. These fascicles were surrounded by a relatively thick epineurium. The remaining channel lumen was devoid of any regenerated tissue structure. The nerve cable area and number of myelinated axons, but not the axonal density, had significantly increased over time in the case of nerves regenerated through NGCs made from DegraPol®/btgc b17. No significant difference in terms of the nerve cable area and the number of myelinated axons and axonal density was detectable over the 24 weeks time period in the case of NGCs made out of DegraPol®/btgc b41 (Table 16 - Table 18). Identically to DegraPol®/btgc b8 NGCs, the inflammatory reaction occuring on the surface of polymer fragments was well separated from the regenerated neural tissue.

Table 16 Mean nerve cable area of regenerated nerves; n.d.: not done.

	mean cable area [mm^2]		
duration of implantation [weeks]:	4	12	24
DegraPol®/btgc b8	0.23 ± 0.05	0.29 ± 0.1	0.26 ± 0.02
DegraPol®/btgc b17	0.13 ± 0.05	n.d.	0.5 ± 0.13
DegraPol®/btgc b41	0.35 ± 0.09	0.23 ± 0.1	0.34 ± 0.05

Table 17 Mean number of axons of the regenerated nerves; n.d.: not done.

	number of axons		
duration of implantation [weeks]:	4	12	24
DegraPol®/btgc b8	3908 ± 436	6967 ± 806	5891 ± 381
DegraPol®/btgc b17	2693 ± 1289	n.d.	11423 ± 2073
DegraPol®/btgc b41	6296 ± 586	6043 ± 2454	7600 ± 1094

Table 18 Mean axon density of regenerated nerves; n.d.: not done.

	mean axon density [1/1000 μm^2]		
duration of implantation [weeks]:	4	12	24
DegraPol®/btgc b8	17 ± 3	24 ± 5	23 ± 3
DegraPol®/btgc b17	20 ± 1	n.d.	23 ± 2
DegraPol®/btgc b41	18 ± 3	26 ± 3	25 ± 3

Polymer Analysis

Average molecular weight. After four weeks of implantation, the weight average molar mass had dropped below 50'000 for all three tested polymers as assessed by GPC analysis. At 12 weeks this value had decreased further, approaching the average molar mass of the starting PHB blocks after 24 weeks (Figure 27). For comparison, the molar mass decrease of polymers degraded in buffered aqueous solutions at pH = 7 and 37 °C, is shown in the same figure. Within the error of measurement, the molar mass decrease shows the same behavior in vivo versus in vitro for all tested polymers. The relatively large differences in starting molar masses levels off after advanced degradation.

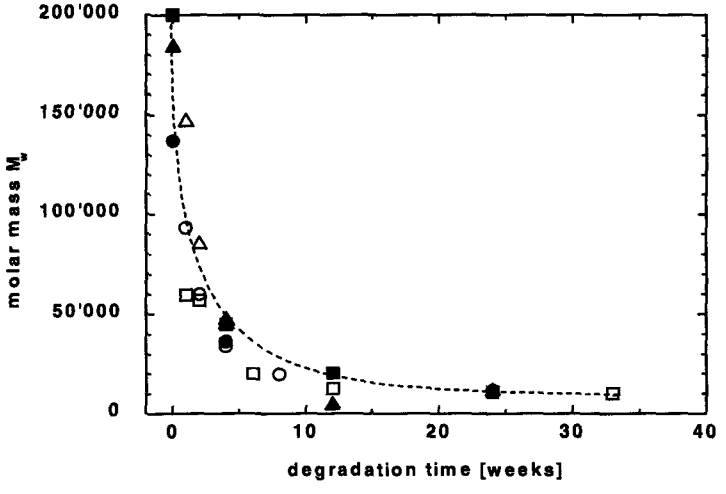

Figure 30 Decrease of the weight average molar mass as a function of degradation time. The open symbols refer to hydrolytic degradation experiments in buffered water solution (pH=7, 37 °C). Plain symbols represent the molar masses of samples implanted for different time periods. (■/□ DegraPol®/ btgc b41; ●/○ DegraPol®/btgc b17; σ /Δ DegraPol®/btgc b8)

Crystallinity. The x-ray diffraction patterns of all polymers show the characteristic signals of crystalline PHB with diffraction peaks at 13.5 ° and at 17.0 °, corresponding to the (020) and (110) planes of the unit cell of crystalline PHB, respectively. With a maximum around 20 °, the broad amorphous halo obscures some distinct signals from the crystalline domains. Figure 6 of chapter 2 shows the diffraction patterns of the used polymers compared to pure PHB blocks. With increasing PHB content, the crystallinity of the polymers is increased, as revealed by the surface ratio of the crystalline peaks to the amorphous halo. For the polymer with initial 41 wt-% of PHB, the crystallinity was followed during the degradation process. Up to 12 weeks of implantation, the crystallinity of that polymer was almost constant. The diffraction pattern shows no changes in the crystalline structure, and all signals can be associated with the crystalline PHB domains (Figure 31). The melting point increased from 120 °C to 130 °C during the

first 12 weeks of implantation. Due to small samples, the early loss of material strength and the low crystallinity with the 8 and 17 wt-% PHB polymers, the crystallinity could not be followed during degradation for these polymers (Figure 32).

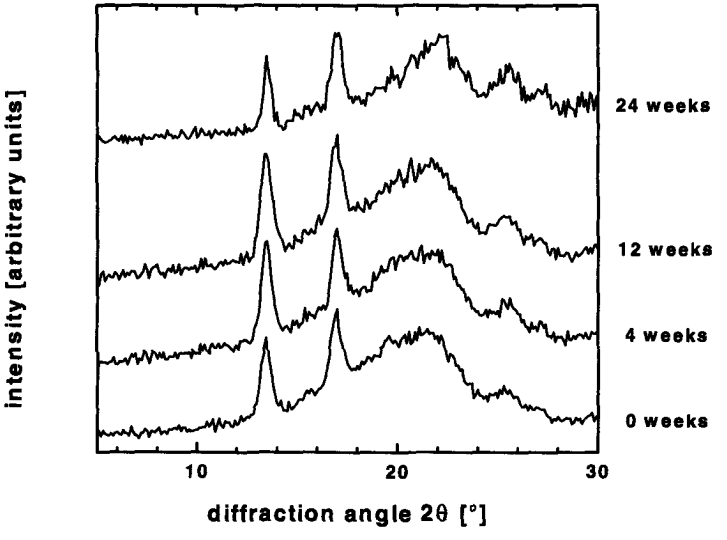

Figure 31 X-ray diffraction pattern of DegraPol®/btgc b41 after different times of implantation.

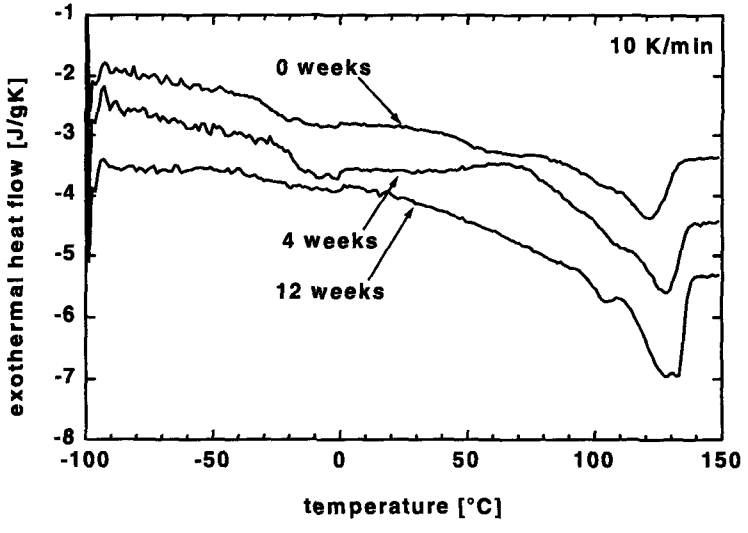

Figure 32 Thermogramms of DegraPol® /btgc b41 after different times of implantation.

Chemical copolymer composition. The relative amount of the major monomer units, butyric acid, e-caprolactone, and glycolide, can be calculated from the ^{1}H-NMR spectra (Table 19). Assuming that the total amount of butyric acid units is constant, the remaining implant mass can be estimated from the monomer unit composition of the polymers after different implantation times (Figure 33 A, B, C). For all polymers, the estimated mass loss started between the 4th and the 12th week of implantation. After 24 weeks of implantation, all polymers had almost the same composition and consisted of about 64 wt-% of PHB, 20 wt-% of e-caprolactone units, and 5 wt-% of glycolide units independently of their starting composition. Taking into account the starting amount of PHB, a total weight loss of 33, 74, and 88 % was resulting for the polymers with initial 41, 17, and 8 wt-% of PHB blocks, respectively.

Microstructure. Before implantation, all tubes presented very smooth inner and outer surfaces. Tube fragments of all polymers, explanted after 24 weeks, had sharp edges

indicating brittle fracture (Figure 34 A, C, E).

Table 19 Changes in chemical composition after polymer implantation; n.d.: not done.

	butyric acid units [wt-%]				ε-caprolactone units [wt-%]				glycolide units [wt-%]				diurethane units [wt-%]			
duration of implantation [weeks]:	0	4	12	24	0	4	12	24	0	4	12	24	0	4	12	24
DegraPol®/ btgc b8	8	8	18	64	57	62	52	18	27	19	21	4	8	11	9	14
DegraPol®/ btgc b17	17	17	n.d.	67	51	51	n.d.	21	24	23	n.d.	5	8	9	n.d.	7
DegraPol®/ btgc b41	41	42	46	62	34	34	33	21	15	14	11	7	10	10	10	10

Within the channel fragments with an initial content of 41 wt-% of PHB-blocks, many cracks were spread all over the surface, apparently following the spherulithical structure of that material (Figure 34 A, B). Around the cracks, small holes could be observed, indicating porosity. In between the cracks, the surface appeared to be still very smooth. The channel fragments of the NGCs with the 8 and 17 wt-% PHB-blocks displayed rougher surfaces but not the same kind of cracks following a spherulithical structure (Figure 34 D, F). The surface roughness is possibly revealing a porous structure of the bulk material. Some smaller cracks of approximately 1 µm opening width were visible.

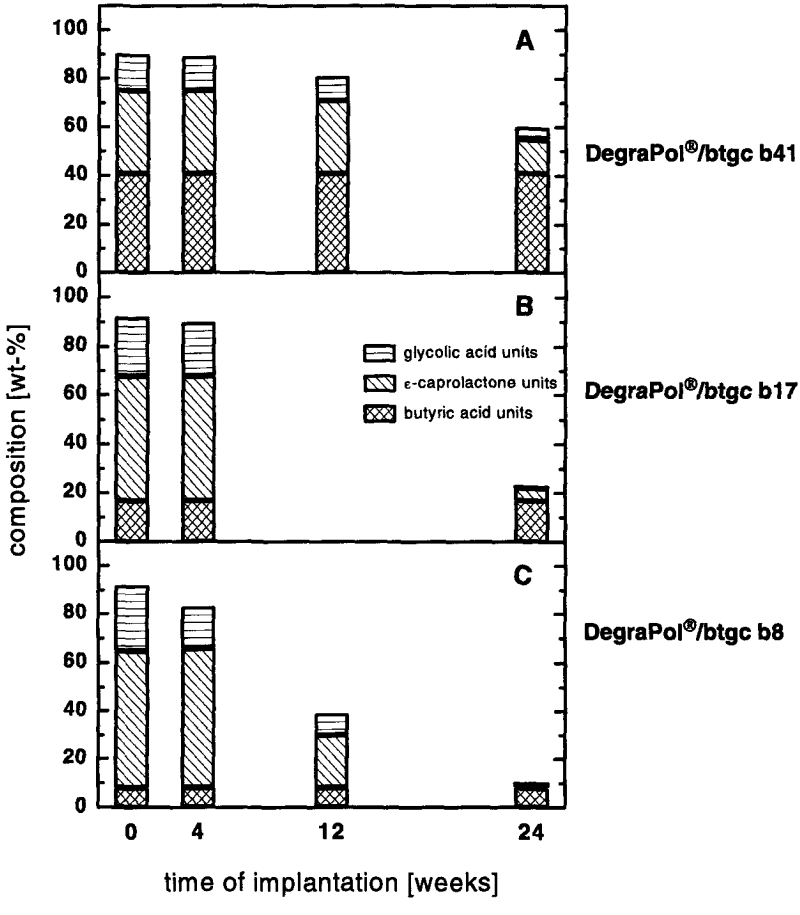

Figure 33 Changes in chemical composition of the polymers indicated after different implantation times. The cross-hatched area of the columns represent the content of butyric acid units, the diagonally striped that of ε-caprolactone units, and the horizontally striped that of glycolid units.

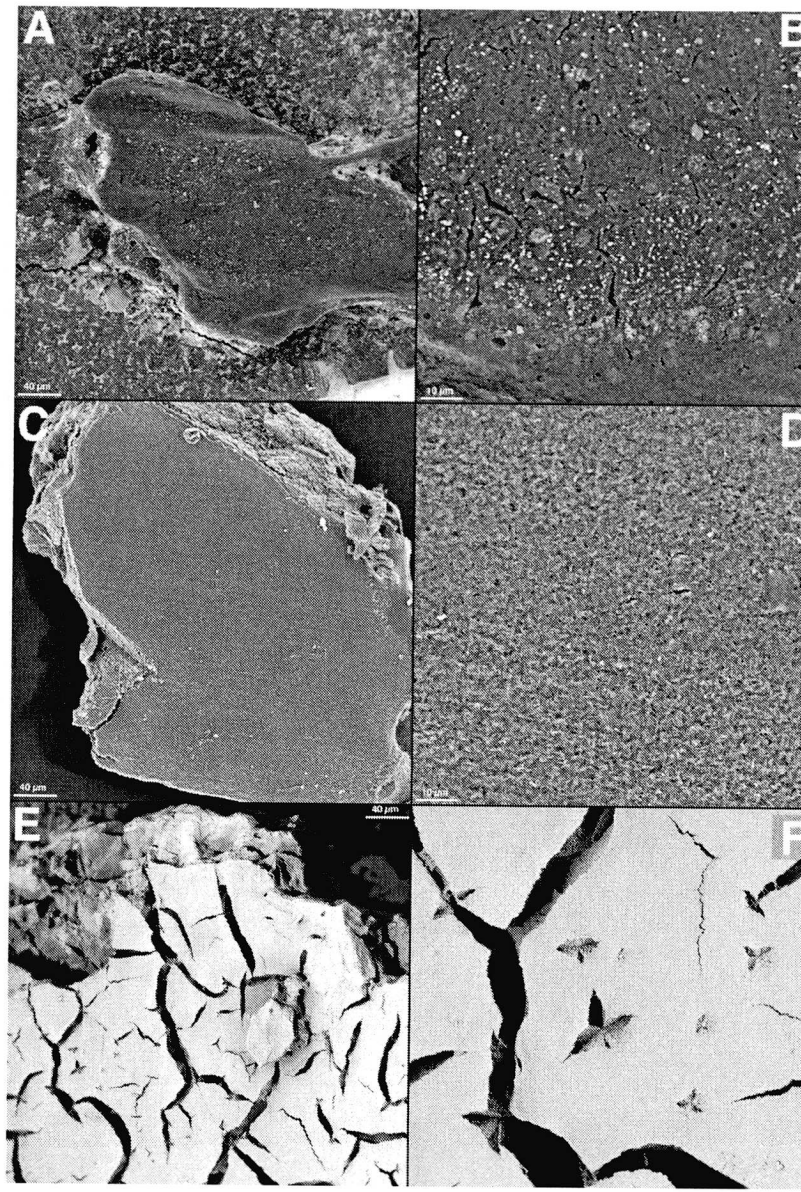
A
B
C
D
E
F
40 µm
40 µm
40 µm

Figure 34 SEM images of surfaces of explanted polymer channels after 24 weeks. DegraPol®/btgc b8 (A) x250, (B) x1000; DegraPol®/btgc b17 (C) x250, (D) x1000; DegraPol®/btgc b41 (E) x250, (F) x1000.

Discussion

Nerve guidance channels fabricated from biodegradable polyesterurethane polymers facilitate nerve regeneration across an 8 mm gap of an axotomized sciatic nerve in the rat. The present study illustrated that this newly developed material did not impede nerve regeneration upon degradation and furthermore could be tailored to meet the desired degradation profiles. This study also shows that low PHB content induces faster degradation rates of the polymer material. The employed material could be extruded into polymeric tubes at given diameters and wall thicknesses. In order to be used as nerve regeneration prostheses, these tubes have to resist the pressure from the surrounding muscles, to keep their lumen open for nerve regeneration. During implantation, both, the external stresses, as well as the implant strength will change. In order to keep the volume of implanted material as low as possible, the wall thickness had to be balanced with the required implant strength. Comparing the polymer analysis results obtained during in vivo degradation with the results of hydrolytic degradation in buffered water solution at pH 7 and 37 °C, a three-step degradation process is suggested:

(I) Hydrolytic chain scission. The polymer degradation started by random chain scission, most probable by hydrolysis of glycolyl-glycolate esters of the soft segments. During this degradation step, the width of the molar mass distribution remained almost constant, whereas the average molar mass decreased by hydrolytic degradation in a similar manner in vitro and in vivo. This molar mass reduction induced a loss of mechanical properties, such as strength, elongation at break or toughness. The chemical composition, detected by ^{1}H-NMR, and the degree of crystallinity were mainly unchanged during this step. This first degradation step described the events occurring during approximately the first 4 weeks.

(II) Resorption of small, water soluble chain fragments. The hydrolysis of soft

segments within the polymer resulted in the generation of small polymer-chain fragments, that became water soluble, leached out of the polymer bulk, and were resorbed. The material loss induced by this process did not occur homogeneously across the bulk of the implant, leading to inhomogenous shrinkage and resulting in internal stress fields. Depending on the material strength and morphology at this time, the stresses were released by the formation of small cracks all over the polymer, as observed in the DegraPol®/btgc b41. Simultaneously, external loads, caused e.g. by muscle contraction, fractured the tube into few large pieces. This degradation step started slowly between the 4^{th} and 12^{th} week of implantation. It was evidenced by the cracks becoming visible upon explantation, by the channel's loss of integrity upon gentle manipulation with surgical forceps, by the small cracks observable under the SEM and by ^{1}H-NMR and XRD results.

(III) Final resorption by inflammatory cells. Once the channel had been reduced to smaller pieces, the inflammatory reaction and the clearing of small polymer fragments was potentially due to a higher surface area. Inflammatory cells at the polymer interfaces were observed in stained hystological cuts of the implantation site after 24 weeks of implantation. (Figure 29) If the implant fragments become small enough, they are phagocytosed by macrophages.[9] This degradation step will continue until total resorption.

As our block copolymers were insoluble in water, entire copolymer chains were very unlikely to be resorbed. Changes in the polymer chains were deduced from the overall monomer unit composition determined by ^{1}H-NMR. The relative loss of glycolide and caprolactone units, starting between week 4 and 12 was therefore associated with the resorption of small polymer fragments as a consequence of repeated chain scission in the polymer "soft segments". The increase in crystallinity started approximately at the same time. The diffraction patterns showed no changes of the crystalline unit cells, as evidenced by the PHB characteristic peaks. Signs of a partial leaching of polymer fragments were also observed with SEM analysis. Cracks of a few micrometers opening and a clearly porous structure were visible. It appeared that the remaining polymer,

mostly crystallizable PHB-blocks, built a structure that supported dimensionally the polymer fragments.

The resorption of implant fragments by inflammatory cell action should be confirmed by *radioactive or fluorescent labelled polymers.* Nevertheless, an increased activity of inflammatory cells was visible after 24 weeks of implantation, especially at the surface of polymer particles, strongly suggesting a cellular component for the material clearance. Indeed macrophages and giant cells were observed trying to remove polymer debris. Assuming the amount of PHB to remain constant, a minimum of 45 to 85 wt-% of the implant material has already been resorbed after 24 weeks of implantation, as can be deduced from the copolymer composition calculated from ^{1}H-NMR spectra of the different polymers. As the PHB crystallinity was approximately 40 wt-%, some of the PHB monomer units may also have been resorbed, increasing the material loss after 24 weeks.

The three tested polymers with 41, 17, and 8 wt-% of PHB-segments represent a set of polymers where just one chemical parameter, the content of crystallizable blocks was changed. This parameter influences the mechanical properties of the polymer, the morphology of the crystalline domains within the polymer, the degradation behavior and potentially the foreign body reaction. The first two steps of degradation, as described above, are quite similar for all three tested polymers leading to an almost complete resorption of non crystallizable blocks of the polymers after 24 weeks of implantation. The polymer DegraPol®/btgc b8 has the minimally needed content of PHB blocks of 8 wt-%, to achieve adequate mechanical properties. After 24 weeks of implantation it had the highest weight loss, the lowest mechanical stability, and is thought to lead to complete resorption within one year.

Nerve Regeneration. The occurrence of large cracks during the first 4 weeks of implantation as in the case of DegraPol®/btgc b8, along the entire length of the channels and the resulting tissue ingrowth did not impede nerve regeneration, as it is believed that the nerve cable formation occurs during the first two weeks. The inflammatory reaction

was localized essentially around channel segments and separated from the nervous tissue preventing any negative interference with the nerve regeneration process. Whether the observed plateau for the number of myelinated axons in the case of DegraPol®/btgc b8 after 24 weeks is a consequence of such an inflammatory reaction has to be examined over longer implantation periods.

Interestingly, the highest mean value for the number of myelinated axons as well as nerve cable area was detected in nerves regenerated through guidance channels fabricated from DegraPol®/btgc b17. Whether the large number of axons is indeed related to the material's composition should be investigated further by augmenting the number of implanted specimen. The degree of regeneration at 4 weeks independent of the PHB concentration is comparable to those obtained by others using a two-ply biodegradable nerve guidance channel out of poly(*L*)lactic acid and a polyester-urethane.[22] Other studies evaluating bioresorbable NGCs were not comparable due to differences in experimental protocols. Earlier investigations using nerve guidance channels made out of non-resorbable polymers such as silicone elastomer reported similar nerve cable morphologies as well as numbers of myelinated axons.[53] Nerve cables were also found to be surrounded by an epineurial tissue layer consisting in several layers of interlaced fibroblasts. Additionally, myelinated axons were organized in groups forming small fascicles.

One can conclude that this polymer system is well suited for the fabrication of nerve guidance channels. The time frame of degradation can be tailored according to its composition and dimensions. Due to its very low degree of swelling and its elastomeric properties the material offers several advantages versus other resorbable polymers used as NGCs to date.[20,22,24] Prior to its clinical use, polymer safety and toxicology studies need to be conducted. In addition, long-term studies aimed at the functional evaluation of the regenerated nerve tissue upon complete elimination of the polymeric material will have to be performed.

CHAPTER 8 *General Discussion*

When this work started, the chemical structure and the synthesis of DegraPol®-polymers had already been improved several times. Synthesis routes for a variety of building blocks and block-copolymers, e.g., with different degradation characteristics were available. Some simple implants had successfully been tested in cell cultures and as subcutaneous implants on rats. The first degradation stages, where basically the molecular weight of the polymer is drastically reduced, had been studied in a laborious work for a great variety of DegraPol®-polymers.[29] The resorption of the expected longest lasting constituents of the polymer material, highly crystalline PHB-particles, had also been investigated.[9] Cell cultures containing fluorescent labelled PHB-particles, have been used to observe the phagocytosis of such particles and their subsequent digestion. Why was an additional work of any use on such a well explored field?

The main goal of the DegraPol®-research was to develop a new, highly useful material for medical applications. The material-development should not stop after the successful synthesis of the material. It should be continued in medical institutions, finally leading to the use of this new materials in medical applications. Probably the most convincing argument for the use of a new material, is to demonstrate its usefulness on a specific application. Such a demonstration is a fundamental prove and is best suited to motivate people from all involved disciplines to work with the new material. This was one reason for the development of nerve guidance channels in this work.

Using DegraPol®-grades for nerve guidance channels increases the empirical knowledge

of how these polymers behave. The two main questions in this context were: Would the nerve regeneration be adversely affected by the DegraPol® nerve guidance channel? And would the polymer degradation and resorption occur as expected from previous investigations? Concerning the first question, based on the obtained results a qualitative answer can be given: The inflammatory reactions were relatively mild, and the nerve regeneration was as good as with other previously used implant materials. Probably, the degradation rate was well balanced with the resorption capacity of the host body and the degradation products did not reach harmful concentrations. The small tube fragments created after advanced degradation, did not cause an excessive inflammatory reaction, as it has been reported for other materials. This may be due to chemical or topological differences between DegraPol® fragments and fragments from other materials. The rate of formation of DegraPol®-fragments may also be important. Both sides of the inflammatory reaction, the implant and the host body, are complex systems. The implant material must be considered as a complex system, as it is continuously changing its surface, its chemical composition and its shape during application. Thus it would have been far beyond the scope of this research to try to influence the biological response by the material design. (see Chapter 7)

As nerve guidance channels, the first used DegraPol®-grades were degraded, but just resorbed to small amounts. This is consistent with the results from previous degradation studies in buffered water solutions and with studies of subcutaneously implanted polymer films. This result was not satisfying, as good material properties were lost due to degradation, but just small amounts of the material were resorbed. Optimizing the materials design, this gap between material degradation and material resorption could be filled by changing the block-length, the block-length distribution, and the relative amounts of the different kinds of blocks within the polymers. (see Chapter 2 and 7)

During this and earlier research, the non crystallizable blocks of DegraPol® were found to be the first parts to be degraded. Parts of the degradation products of the non crystallizable blocks were dissolved during degradation studies in buffered water. After this relatively fast degradation-step, a solid material of low molecular weight polymer

(M_w = 10'000) remained and was almost not further degraded. At this degradation stage, the previously used DegraPol®-grades still maintained a sufficiently high strength to prevent them from falling apart into small particles. A basic assumption of this work was if the implant material would disintegrate into small particles of some micrometers size, the slowest degrading, highly crystalline parts of the polymer would be phagocytosed, leading to total polymer resorption within time-periods of some months. This assumption was supported by the phagocytosis-investigations on fluorescent labeled PHB-particles, done in earlier research. A reduction of the relative amounts of PHB within the polymer should isolate the PHB-domains, reduce the connectivity of these domains, and thus drastically lower the strength of the low molecular weight material, remaining after advanced degradation of the former DegraPol®-grades. Narrowing the size-distribution of the PHB-diols by fractional precipitation, should cause the domain-formation in the polymer to improve, as known for polyurethanes. The amount of PHB needed for mechanical stability of the polymers was reduced in that way and the set of DegraPol®-polymers could be extended to polymers containing as little as 8 wt-% of PHB. (see Chapter 2)

The mass loss after longer periods of implantation was not trivial to be determined for these polymers because the material degradation lead to a drastic embrittlement of the implant material and made handling difficult. A gravimetric measurement of the remaining implant mass was not possible, as major parts of the implant may have been lost during explantation and cleaning. The implant fragments were porous, as could be seen on electron micrographs. A volumetric determination of the polymer resorption was therefore not possible. Nevertheless, the chemical composition, determined by NMR, could be used to estimate the mass loss after different periods of implantation. The determined relative content of hydroxybutyric acid-units in the polymers increased with the time of implantation. This must be due to a faster resorption of glycolide- and ε-caprolactone units from the polymer. Assuming that no hydroxybutyric acid-units were resorbed, the mass loss of the whole implant can be estimated from the changes of the chemical composition of the implant. This method is unique to polymers, where slowly degrading components of the implant material can be distinguished and quantified. It

revealed to be a highly useful method to determine the mass loss of highly resorbable polymers. (see Chapter 7)

SEM-pictures of etched polymer surfaces were used to get an idea of the domain structure in the polymers. These pictures suggest that the materials were build up of connected crystalline lamellas with a continuous domain filling the volume in-between. The distance between the lamellas was bigger in the polymers containing low amounts of PHB. A detailed investigation, e.g. by transmission electron microscopy on stained polymer samples, seemed to be too laborious for this stage of polymer development. The purities of the amorphous domains were estimated from the steepness of the steps in the DSC-curve, associated with the glass transition. The width of the loss factor peaks of dynamic mechanical measurements were interpreted in the same way. Polymers made from fractionated PHB-blocks caused sharper signals and are therefore thought to have amorphous domains of higher purity. The high degree of resorption after 24 weeks of implantation, estimated to 88 % for DegraPol®/btgc b8, was for the moment satisfactory. Further investigations to prove the above mentioned ideas on the relation between material design and material resorption could be conducted in future.

DegraPol®-polymers were designed to be processable through standard processing routes of thermoplastics. In the present study, this was proven by melt-extruding the pure polymers from a laboratory made plunger extruder. The plunger-extruder design was well suited for the small quantities of polymers available. If bigger quantities were available, a screw-extruder design would be adequate. The advantages would be the continuous process with constant residence times of the polymer in the heating zones, and the higher homogenization of the polymer melt in the extruder. The higher shear-stresses in screw-extruders are possible disadvantages. The extrusion could easily be adapted for the production of some dozens of meters of polymer tube per day. This would result in thousands of 10 mm long nerve guidance channels, just with one medium size extruder. - A veritably elegant production line! All other standard processing methods of thermoplastics, including processing through solutions, should also easily be possible. (see Chapter 4)

The good collaboration of research groups from different areas was essential for the presented type of research. Synergistic effects were achieved by an intensive collaboration between a laboratory of macromolecular chemistry and a division of surgical research. Both partners, the surgical research lab and the macromolecular-chemistry research lab, could concentrate on their core research topics and exchange results in frequent meetings to pursue the common goals.

At the current stage, the developed degradable nerve guidance channels are simple tubes made of a special material, DegraPol®. They could be further developed, e.g. by adding nerve growth factors into a coating of the inner tube surface. The tubes could also be filled with a structure such as a gel or an open porous foam, to support the regenerating nerve. The degradation profile of the implant material could be changed, using a laminated structure. A relatively stable outer layer could be used to protect a faster degradable core of the tube wall. Once the protecting layer would be destroyed, the whole channel would be degraded with the fast degradation rate of the core material.

Conclusion

The initial goal, the realization of a medical application for DegraPol®, was reached up to a stage of successful animal testing. At this stage, one can conclude that the tested polymers are well suited for the fabrication of nerve guidance channels. Prior to its clinical use, further studies need to be conducted to ensure polymer safety and successful functional nerve regeneration.

The present grades of DegraPol® not only loose their good mechanical properties when they degrade, they are also resorbed to their greatest part. The fastest degrading DegraPol®-grades presented, are likely to be fully resorbed within one year of implantation. (This may be confirmed in a last-minute result.) In that respect, one of the initial development-concepts of DegraPol® could be realized: the complete resorption of DegraPol® in several steps. The first step being the resorption of water soluble degradation products, the last step the resorption of highly crystalline PHB-particles

under the influence of body cells.

The size distribution of PHB-diols was narrowed by an additional fractional precipitation step. This lead to the desired improvement of the polymer properties. A slight change of the conditions during alcololysis of PHB and purification of the PHB-diols could lead to the same result as the subsequent fractional precipitation introduced during this work. This would improve some properties of DegraPol® without complicating the polymer synthesis.

The used DegraPol®-grades could be processed to slender tubes in a simple extrusion process. For a better control of the tube dimensions, a drawing device enclosing the tube after the die would ease the production of tubes, especially at low wall thicknesses. This would reduce the amount of scrap and thus the production costs.

CHAPTER 9

Experimental Part

Materials

The following reagents and solvents were purchased from Fluka (Buchs, Switzerland) in the indicated grades: ethanol puriss., diglyme (bis[2-methoxyethyl]ether) puriss., ethylene glycol puriss., dimethyl sulfoxide purum, tetrahydrofurane purum, hexane fraction purum, ε-caprolactone purum, dibutyl tinoxide purum, dibutyltin dilaurate pract. From Scharlau (Barcelona, Spain), dichloro ethane >99.5 %, from Riedel de Haën (Seelze, Germany), methanol >99.8 %, from J.T. Baker (Deventer, Holland), acetone >99.5 %, from Hüls (Küsnacht, Switzerland) trimethyl hexamethylene diisocyanate (TMDI) as an isomeric mixture of 2,2,4-TMDI and 2,4,4-TMDI, from Boehringer (Ingelheim, Germany), diglycolide, and from ICI, Inc. (Cleveland, UK) poly[(*R*)-3-hydroxybutyrate-*co*-(*R*)-3-hydroxyvalerate] (PHB) as technical grade Biopol™ polyester, poly[ε-caprolactone]-diol M_n=1250, from Polysciences Inc. (Warrington, PA) were purchased.

Solvents

1,4-dioxan puriss and dimethyl sulfoxide purum were purchased from Fluka (Switzerland)

Methods

Molecular Weights

Molecular weights and molecular weight distributions of the polymers were determined by size-exclusion chromatography (GPC) in tetrahydrofurane (THF) on a PLGel mixed C 5 μm column. The instrument (Knauer) was equipped with a small-angle light scattering detector (Chromatix KMX6), a differential-refractometry detector (Knauer DRI), and a viscosimetry detector (Viscotek Differential Mod. # 502). A universal calibration with polystyrene standard samples was applied. The number average molar mass of the initial building blocks was determined by means of vapor phase osmometry, at 25 °C in dichloromethane, or at 40 °C in 1,2-dichloro ethane, on a CORONA WESCAN C32A instrument. Estimated error of molecular weight measurements: ±10 %.

X-Ray Diffraction

For the wide angle X-ray diffraction (WAXD) investigations, a four-circle Siemens D500 diffractometer equipped with a graphite flat-crystal monochromator, nickel-filtered CuK_α radiation (40 kV, 35 mA), pinhole collimation, and a scintillation counter was used. Diffraction patterns were taken at room temperature with a step size of 0.1 ° in 20 or 40 second time intervals.

Scanning Electron Microscopy

Scanning electron microscope images were taken using a Hitachi S900 low-field emission electron microscope, at 10 kV, 4.6 mA acceleration current. Samples were shadowed with 3 nm Platinum under an angle of 45 ° and covered with 5 nm of Carbon under sample rotation. Backscattered electrons were observed.[54] Porous-walled tubes were immerged into an 80 % aqueous ethanol solution, frozen in liquid nitrogen and broken perpendicular to the tube axis for sample preparation. Homogeneous samples were either cut at room temperature or fractured in liquid nitrogen.

Processing to Open Porous Foams

Open porous DegraPol® structures have been recently developed using a solution processing technique.[5] A DegraPol® solution was casted into a stainless steel well, cooled to form a gel and frozen below the melting point of the solution and below the glas transition temperature of the polymer, carefully controlling the temperature and the duration of each step. The so obtained frozen gels were freeze dried to remove the solvent from the gels and to gain open porous polymer foams. Here, 5 wt-% solutions in 1,4-dioxan were let to form gels at 12 °C for 18 hours. The gels were then first cooled down to 5.5 °C for 2 hours, secondly to 3 °C for 1 hour, and to -4 °C for 1 hour. Finally the already frozen solutions were quenched in liquid nitrogen and freeze dried at 10^{-5} bar for 18 hours.

The obtained foams were immerged into an 10 % aqueous solution of ethanol, frozen, and cut into 1.5 mm thick slices. Two slices of each type of foam were sputtered with 30 nm of tungsten for electron microscope imaging of the foam morphology.

Tensile Test of Porous-Walled Tubes

Dry specimens of the porous walled tubes were mechanically tested at room temperature on a Mecmesin M1000E tensile tester. 12 mm long pieces were clamped into the heads of the tensile tester. The free sample length was 5 mm. The tests were run at a constant strain rate of 0.02 s^{-1} and stress-strain curves were recorded until specimen rupture.

Tensile Test of Homogeneous Samples

Tensile tests were carried out on a Mecmesin M 1000E with a load cell capable of measuring forces up to 10 N on dog-bone-shaped samples measuring 5 (free length) x 3 x 0.15 mm, and with a strain rate of 0.2 s^{-1} at room temperature.

Estimated errors:

Young's Modulus: ±10 %

Yield strength: ±10 %

Elongation at break: ±30 %

Dynamic Mechanical Measurements

The storage modulus E', and the loss modulus E", were determined on compression-molded films with a Polymer Laboratories DMTA MKII using a combined head in the tensile mode, applying a sinusoidal strain with 1 Hz frequency and 0.2 % peak-to-peak strain amplitude. Samples were kept stretched under a constant tensile force of 0.7 N. The Temperature was varied from -100 °C to 130 °C with a heating rate of 2 °C/min.

Differential Scanning Calorimetry

Melting points, glass transition temperatures, and melting enthalpies were determined on a Mettler DSC 30 differential scanning calorimeter equipped with a low-temperature cell and with a TC11 TA 4000 processor at a heating rate of 10 °C/min; indium was used for calibration.

Estimated errors:

Glass transition temperature, melting point: ±2 °C

Contact Angles

For the determination of the contact angle of water on the polymer surfaces, a Ramé-Hart 100-00 goniometer was used. Contact angles were measured in two ways: The advancing contact angle of water was measured after adding two portions, each of 3 µl, of water to the polymer surface, pre-conditioned for 7 days in vacuo; the contact angles of air in water were measured by placing an air bubble underneath a polymer coated glass slide placed horizontally in a transparent water container.

Estimated error: ± 5 °

Nuclear Magnetic Resonance

The NMR spectra were either measured on a BRUKER AM 300 WB or on a BRUKER Avance DPX 300 at 300 K in DMSO-d_6 with tetramethylsilane as reference. Spectra were analyzed using peak assignations published in previous papers.[7,8]

Estimated errors:

all compositions determined by ^{1}H-NMR: ± 5 %

Size Selective Permeability

2 cm long porous walled tubes were filled with 20 % aqueous dextrane solutions and closed at both ends with a drop of epoxy-glue. The permeability of dextrane molecules with a molar mass of 6'000 was compared with that of dextrane molecules of 70'000 molar mass. Tubes filled with pure water were submitted to the same treatment for control. The filled tubes were then placed in 4 ml of deionized water. To determine the dextrane diffusion through the tube wall, the dextrane concentration in the surrounding water was measured by UV absorption measurements at 300 nm after 5 days.

Synthesis

Telechelic OH-terminated poly{[(*R*)-3-hydroxybutyric acid]-*co*-[(*R*)-3-hydroxyvaleric acid]} (PHB-diol) with a number-average molar mass between 2000 and 3000, containing 5 wt-% hydroxyvaleric acid units, was prepared by transesterification of bacterial, high-molecular-weight PHB with ethylene glycol following the method of Hirt, Neuenschwander and Suter.[7] Non-crystallizable telechelic OH-terminated poly[glycolid-*co*-(ε-caprolactone)] was prepared as low-molecular-weight, random copolymer, following the synthesis of Lendlein, Neuenschwander and Suter,[8] by ring opening co-polymerization of diglycolid and ε-caprolactone with ethylene glycol in the presence of dibutyltinoxid as catalyst. The final molar mass was defined by the molecular ratio of the ring-opening initiator ethylene glycol to the cyclic esters diglycolid and ε-caprolactone and was chosen to be about 3000. The two OH-terminated segments described above were dissolved in the desired ratio in 1,2-dichloroethane and chain extended with 2,2,4-trimethyl hexamethylene diisocyanat, using the synthesis, isolation and purification procedure described by Hirt, Neuenschwander and Suter.[3]

For the sake of simplicity, a suffix is added to the family of copolymers termed collectively DegraPol®/*hjs* **bx**, where *h* indicates the type of crystallizable blocks, *j* the type of junction unit, *s* the type of non-crystallizable blocks, and *x* the content of

crystallizable blocks. The polymers described here have the following suffix: the crystallizable blocks are denoted by a **b** (from polyhydroxybutyrate), the junction unit by a **t** for TMDI, the non-crystallizable blocks by a **gc** for poly[glycolid-co-(ε-caprolactone)] or by a **c** for poly[ε-caprolactone]. A copolymer prepared with the above components, having 17 wt-% of hard segment would be named: DegraPol®/btgc **b**17.

Recristallization of PHB-diol

Low molecular weight PHB-diols, obtained as mentioned above, were fractionated by precipitation. About 0.5 grams of a fine powder of PHB-diol (M_n = 2200) was suspended in 20 g of a solvent and refluxed under permanent stirring until the PHB was completely dissolved. If the suspension was not completely clear, the suspension was stirred at the boiling temperature for 10 hours. The solution (or suspension) was then slowly cooled within 4 hours to room temperature and let to precipitate during 12 hours. The precipitate was isolated by filtration trough a 4 μm glass filter and dried in vacuo before determining its weight. The solvent of the filtrate was evaporated and the mass of the dissolved fraction was determined after drying in vacuo. Solutions where all PHB-diol remained soluble at room temperature were cooled down to 2 °C and let to precipitate during 12 hours.

Hydrolysis Experiment

Extruded polymer tubes of about 10 ± 2 mm length, 0.12 ± 0.05 mm wall thickness and 5 ± 1 mg weight were immersed in 5 ml of phosphate-buffered water solution (pH = 7, 0.2 M) and kept at 37 ±0.5 °C under gentle shaking. Natriumazid (30 mg/l) was added to the water as a bacteriostaticum. After different time intervals, the average molar mass, the monomer unit composition, the crystallinity, and the dimensions of the samples were determined. For SEM investigation of degraded polymers, 0.15 mm thick melt cast films were immersed into buffered water solution under the above mentioned conditions.

Surface-Etching

Extruded tube samples were etched for different times with a solution of 40 % methylamine in H_2O at 37 °C. The samples were then rinsed three times with deionized water, dried in vacuo and prepared for SEM analysis. A similar etching technique has been used and described for the removal of the amorphous parts on polyhydroxybutyrate (PHB) crystals. The suggested chemical reaction is an aminolysis of the esterbonds by methylamine, attacking the amorphous parts of the polymer faster than the crystalline ones, thus revealing the crystalline structure.[52]

Cell Compatibility Testing

Cells were cultured in polystyrene flasks (Falcon, Inotech Dottikon, Switzerland) in a humidified atmosphere at 5 % CO_2. Macrophages (murine macrophage cell line, J774) were maintained in Dulbeco's modified eagle medium (DMEM) supplemented with 2 g/l $NaHCO_3$, 25 mM HEPES, 10 % fetal calf serum (FCS), 2 mM L-glutamine and 50 µg/ml gentamycin. Fibroblasts (mouse fibroblast cell line, 3T3) were cultured in RPMI 1640 medium supplemented with 2 g/l $NaHCO_3$, 25 mM HEPES, 10 % fetal calf serum, 2 mM L-glutamine and 50 µg/ml gentamycin. Osteoblasts (rat cell line, MC3T3) were maintained in α-modified eagle medium (α-MEM) supplemented with 10 % FCS and 50 µg/ml gentamycin.

For the determination of the cell compatibility during polymer degradation, melt-cast polymer films were degraded for different time intervals at 37 °C in culture medium filled wells of a 24-well tissue-culture plate. The culture medium was removed with the soluble degradation products and cells were added to the polymers at a density of 5×10^4 cells per well in 1 ml of their respective culture medium. The cell density on the polymers was determined four days after cell seeding using the MTT test. As positive control, cells were platted onto 24-well tissue culture plates. NO levels in the supernatant of macrophages (J774) cultured on the test polymers were determined using Griess reagent. The morphological integrity of the cells was controlled by scanning electron imaging.

References

1 H. Plank, "Kunststoffe und Elastomere in der Medizin", Verlag W. Kohlhammer, Stuttgart, 1993

2 B. Saad, O. M. Keiser, M. Welti, G.K. Uhlschmid, P. Neuenschwander, U.W. Suter, "Multiblock Copolyesters as Biomaterials: In Vitro Biocompatibility Testing", *J. Mat. Sci.: Mat. in Med.*, in press

3 B. Saad, T. D. Hirt, M. Welti, G.K. Uhlschmid, P. Neuenschwander, U.W. Suter, "Development of Degradable Polyesterurethanes for Medical Applications: In Vitro and in Vivo Evaluations.", *J. of Biomed. Mat. Res.*, **36**, 65-74, (1997)

T.D. Hirt, P. Neuenschwander, U.W. Suter,"Synthesis of degradable, biocompatible, and tough block-copolyesterurethanes." *Macromol. Chem. and Phys.*, submitted;

4 M. Borkenhagen, R. C. Stoll, P. Neuenschwander, U. W. Suter, P. Aebischer, "In Vivo Performance of a New Biodegradable Polyesterurethane System Used as a Nerve Guidance Channel.", *Biomaterials*, submitted

5 B. Saad, S. Matter, G. Ciardelli, G. K. Uhlschmid, M. Welti, P. Neuenschwander, U. W. Suter, "Interactions of Osteoblasts and Macrophages with Biodegradable, and Highly Porous Polyesterurethane Foam and its Degradation Products." *J. Biomed. Mater. Res.*, **32**, 355-366, (1996)

B. Saad, G. Ciardelli, S. Matter, M. Welti, G. K Uhlschmid, P. Neuenschwander, U. W. Suter, "Degradable and Highly Porous Polyesterurethane Foam as Biomaterial: Long-Term Effects and Phagocytosis of Degradation Products in Osteoblasts." *J. of Biomedical Mat. Res.*, submitted

6 C. Grob, internal communications

7 T. Hirt, P. Neuenschwander, U. W. Suter, "Telechelic Diols from Poly[(*R*)-3-hydroxybutyric acid] and Poly{[(*R*)-3-hydroxybutyric acid]-*co*-[(R)-3-hydroxyvaleric acid]}", *Macromol. Chem. Phys.*, **197**, (1996), 1609-1614

8 A. Lendlein, P. Neuenschwander, U.W. Suter, "Tissue-Compatible Multiblock-Copolymers for Medical Applications, Controllable in Degradation Rate and Mechanical Properties.", *Macromol Chem Phys*, submitted

9 G. Ciardelli, B. Saad, T. Hirt, O. Keiser, P. Neuenschwander, G. K. Uhlschmid, U. W. Suter, "Phagocytosis and biodegradation of short-chain poly[(R)-3-hydroxybutyric acid] particles in macrophage cell line." *J. Mater. Sci: Mater. Med.*, **6**, 725-730, (1995)

B. Saad, G. Ciardelli, S. Matter, M. Welti, G.K. Uhlschmid, P. Neuenschwander, U.W. Suter, "Cell Response of Cultured Macrophages, Fibroblasts, and Co-Cultures of Kupffer Cells and Hepatocytes to Particles of Short-Chain Poly[(*R*)-3-hydroxybutyric acid]." *J. Mater. Sci: Mater. Med.*, **7**, 56-61, (1996)

B. Saad, G. Ciardelli, S. Matter, M. Welti, G.K. Uhlschmid, P. Neuenschwander, U.W. Suter, "Characterization of the Cell Response of Cultured Macrophages and Fibroblasts to Particles of Short-Chain Poly[(*R*)-3-hydroxybutyric acid]." *J. Biomed. Mat. Res.*, **30**, 429-439, (1996)

G.L. Ciardelli, B. Saad, P. Neuenschwander, U.W. Suter, "Synthesis of Fluorescence-labelled Short-chain Polyester Segments for the Investigation of Bioresorbable Polyesterurethanes.", *Macromol. Chem. Phys.*, **198**, 1481-1498, (1997)

G. Ciardelli, K. Kojima, P. Neuenschwander, U.W. Suter, "Synthesis of biomedical, fluorescence-labelled polyesterurethanes for the investigation of their degradation." *Macromol Chem Phys*, submitted.

10 unpublished data

11 P.J. Barham, A. Keller, E.L. Otun, P.A. Holmes, *J. Mater. Sci.* **19**, 2781(1984)

12 K.E. Sykes, T.J. McMaster, M.J. Miles, P.A. Barker, P.J. Barham, D. Seebach, H.-M. Müller, U.D. Lengweiler, *J. Mater. Sci.* **30**, 623 (1995)

13 C. D. Eisenbach, M. Baumgartner, C. Günter, *Advances in Elastomer and Rubber Elasticity*, **51**(1986)

14 M. Merle, A.L. Dellon, J.N. Campell, P.S. Chang, "Complications from silicon polymer intubulation of nerves." *Microsurg* **10**, 130-133, (1989)

15 S.J. Archibald, J. Shefner, C. Krarup, R.D. Madison, "Monkey median nerve repaired

by nerve graft or collagen nerve guide." *J Neurosci.*, **15**, 4109-4123 (1995)

16 P. Aebischer, A.N. Salessiotis, S.R. Winn, "Basic fibroblast growth factor released from synthetic guidance channels facilitates peripheral nerve regeneration across long nerve gaps." *J Neurosci Res*, **23**, 282-289, (1989)

17 V. Guénard, N. Kleitman, T.K. Morrissey, R.P. Bunge, P. Aebischer, "Syngeneic Schwann cells derived from adult nerves seeded in semipermeable guidance channels enhance peripheral nerve regeneration." *J Neurosci*, **12**, 3310-3320, (1992)

18 M. Borkenhagen, J-F. Clémence, H. Sigrist, P. Aebischer, "Three-dimensional extracellular matrix engineering in the nervous system." *J Biomed Mater Res.* in press.

19 M. Merle, A.L. Dellon, J.N. Campell, P.S. Chang, "Complications from silicon polymer intubulation of nerves." *Microsurg*, **10**, 130-133, (1989)

20 R. Madison, R.L. Sidman, E. Nyilas, T-H. Chiu , D. Greatorex, "Nontoxic nerve guide tubes support neovascular growth in transected rat optic nerve." *Exp Neurol*, **86**, 448-461, (1984)

21 H.J. Hoppen, J.W. Leenslag, A.J. Pennings, B. van der Lei, P.H. Robinson, "Two-ply biodegradable nerve guide: basic aspects of design, construction and biological performance." *Biomaterials*, **11**, 286-290, (1990)

22 P.H. Robinson, B. van der Lei, H.J. Hoppen, J.W. Leenslag, A.J. Pennings, P. Nieuwenhuis, "Nerve regeneration through a two-ply biodegradable nerve guide in the rat and the influence of ACTH-9 nerve growth factor." *Microsurg*, **12**, 412-419, (1991)

23 C.P. Tountas Bergman, R.A. Lewis, T.W. Stone, J.D. Pyrek, H.V. Mendenhall, "A comparison of peripheral nerve repair using an absorbable tubulization device and conventional suture in primates." *J Appl Biomater*, **4**, 261-268, (1993)

24 W.F.A. den Dunnen, B. van der Lei, J.M. Schakenraad, "Long-term evaluation of nerve regeneration in a biodegradable nerve guide." *Microsurg*, **14**, 508-515, (1993)

25 W.F.A. den Dunnen, B. van der Lei, P.H. Robinson, A.J. Pennings, J.M. Schakenraad, "Biological performance of a poly(lactic acid-e caprolacton) nerve guide: Influence of tube dimensions." *J Biomed Mater Res*, **29**, 757-766, (1995)

26 W.F.A. den Dunnen, I. Strokroos, E.H. Blaauw, A. Holwerda, A.J. Pennings, P.H. Robinson, J.M. Schakenraad, "Light-microscopic and electron-microscopic evaluation of short-term nerve regeneration using a biodegradable poly(DL-lactide-e-caprolacton) nerve guide." *J Biomed Mater Res*, **31**, 105-115, (1996)

27 G. Favaro, M.C. Bortolami, S. Cereser, "Peripheral nerve regeneration through a novel bioresorbable nerve guide." *ASAIO J*, **36**, M291-4, (1990)

28 D.S. Utley, S.L. Lewin, E.T. Cheng, A.N. Verity, D. Sierra, D.J. Terris, "Brain-derived neurotrophic factor and collagen tubulization enhances functional recovery after peripheral nerve transection and repair." *Arch Otolaryngol Head Surg*, **122**, 407-413, (1996)

29 A. Lendlein, PhD Thesis No. 11789, ETH Zurich, (1996)

30 R. C. Stoll, P. Neuenschwander, M. Borkenhagen, U.W. Suter, "Synthesis and Characteriszation of DegraPol® for Nerve Guidance Channels", in preparation.

31 R. C. Stoll, Diploma Thesis, ETH Zurich, (1993)

32 J. Brandrup and E.H. Immergut (Ed.), *Polymer Handbook*, John Wiley & Sons, 3rd ed, New York (1989).

33 H. M. Müller, PhD-Thesis No.9685 , ETH Zürich, (1992)

34 J. Cornibert,R. H. Marchessault, *J. Mol. Biol.* **71**, 735, (1972)

35 M. S. Reisch, *C&EN*, **74** (32), 10 (1996)

36 M. Takayanagi, Mem. Fac. Eng. Kyushu Univ., **23**, 41(1963); M. Takayanagi, I. Imada, T. Kajiyama, *J. Polymer Sci.*, C., **15**, 263 (1966)

37 R.W. Gray, N.G. McCrum, *J. Polym. Sci., Part A2* **7**, 1329 (1969)

38 P. J. Flory, N. Rabjohn, M. C. Shaffer, *J. Poly. Sci.*, **4**, 225, (1949)

39 E. Wetterer, T. Kenner, "Grundlagen des Arterienpulses", Springer-Verlag, Berlin, (1968)

40 L.G. Brazier, "On the flexure of thin cylindrical shells and other thin sections", *Proceedings of the Royal society of London*, Series A, **116**, 104-114, (1927)

41 H. H. Lausberg, "Die Biegestabilität langer dünnwandiger kreiszylindrischer Schalen: Der Brazier Effekt", PhD-Thesis, Univ. Stuttgart, 1977

42 S. Timoshenko, "Strength of Materials", Part 1, D. Van Nostrand Company, Princeton, (1955), 3rd ed.

43 E. Wetterer, T. Kenner, "Grundlagen des Arterienpulses", Springer-Verlag, Berlin, (1968)

44 I.G. Kidson, W.M. Abbott, "Low Compliance and Arterial Graft Occlusion", Circulation, **Suppl. I**, I1 - I4, (1978)

45 W. Hoppe, W. Lohmann, H. Markl, H. Ziegler, "Biophysik", 12th ed., Springer-Verlag, Berlin, (1982)

46 "Extrusion Dies for Plastics and Rubber", W. Michaeli, Hanser Publishers Munich, (1992)

47 B. Saad et al., see ref. 2, 3, 5, and 9

48 T.D. Hirt, PhD Thesis No. 11088, ETH Zurich, 1995

49 O. M. Keiser, PhD Thesis No. 11265, ETH Zurich, 1995

50 G. Ciardelli, PhD Thesis No. 11919, ETH Zurich, 1996

51 S. Matter, PhD Thesis No. 12087, ETH Zurich, 1997

52 S. J. Organ, P. J. Barham, *J. Mater. Sci. Letters*, **8**, 621, (1989)

53 C-B. Jenq, R.E. Coggeshall, "Numbers of regenerating axons in parent and tributary peripheral nerves in the rat." *Brain Res*, **326**, 27-40, (1985)

54 Paul Walther, internal comunication

Curriculum Vitae

Personal Data

Date of Birth	October 16, 1968
Place of Origin	Schaffhausen and Osterfingen SH

Education

1994 - 1997
Institute of Polymers, Department of Materials, Swiss Federal Institute of Technology (ETH), Zurich, Ph. D. thesis

1993 -1994
University Pierre et Marie Curie, Paris, Masters degree in Chemistry and Physical Chemistry of Polymers, (Diplôme d'Etudes Approfondies)

1988 -1993
Department of Materials, ETH Zurich, 3rd. year at ETH Lausanne Diploma (Dipl. Werkstoff.-Ing. ETH)

1981-1987
High School in Zurich and Wetzikon, Matura Type C

1975 -1981
Primary School in Zurich

Professional Experience

since 1997
Istag AG, Egliswil

1993 - 1995
Application programming for the Union Bank of Switzerland, as an employee and as a free-lancer

1991 (3 months)
Visiting Scientist at Massachusetts Institute of Technology

1989 - 1990
Practical training at Huber & Suhner, Pfäffikon (6 weeks) and at Asea Brown Boweri, Baden (6 weeks)

Honors

1993
Award for excellent diploma-thesis (Kunststoff-Technik Preis)

1991
Winner of the invention-contest, Department of Materials, ETH Lausanne

Appendix: Drawings of Special Lab-Equipment

- Plunger extruder assembly, front view, side view, top view
- Draw-wheel set up of the plunger extruder
- Plunger and heating cylinder
- Heating jacket
- Tube die, for small tube-diameters
- Tube die, for large tube-diameters
- Cooling nozzle
- Passive draw-wheel
- Active draw-wheel
- Draw-wheel-lever
- Draw-wheel-block
- Tube welding rig
- Heating-block of the tube welding rig
- Heating- and cooling device for the x-Ray diffractometer
- Heating- and cooling device, assembled in a small scale tensile tester

Plunger extruder assembly, front view, side view, top view

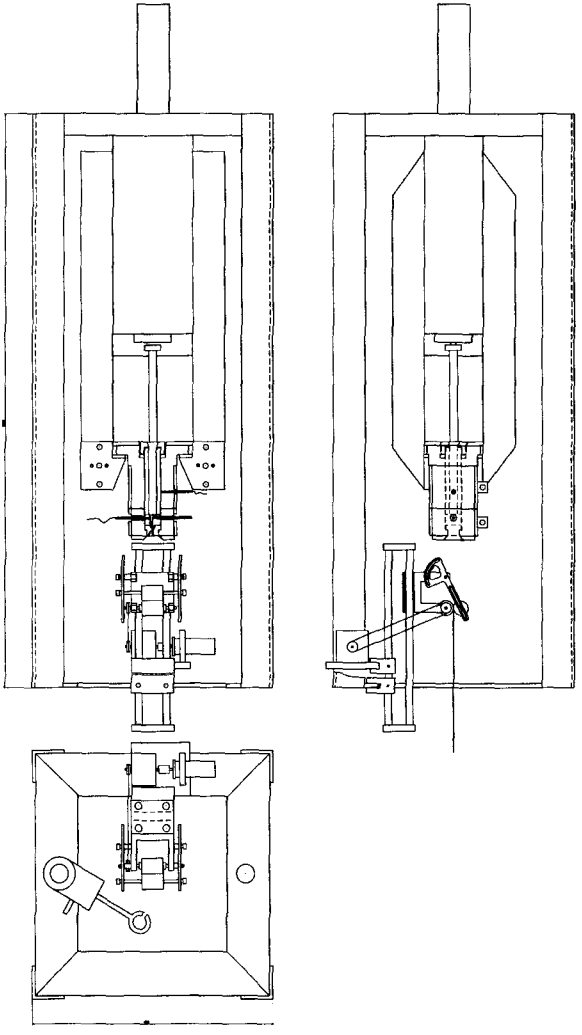

Draw-wheel set up of the plunger extruder

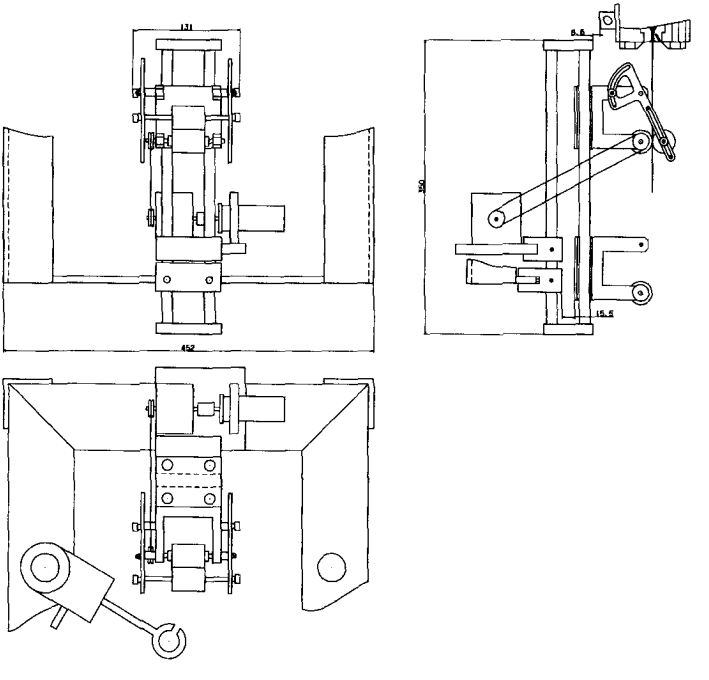

Plunger and heating cylinder

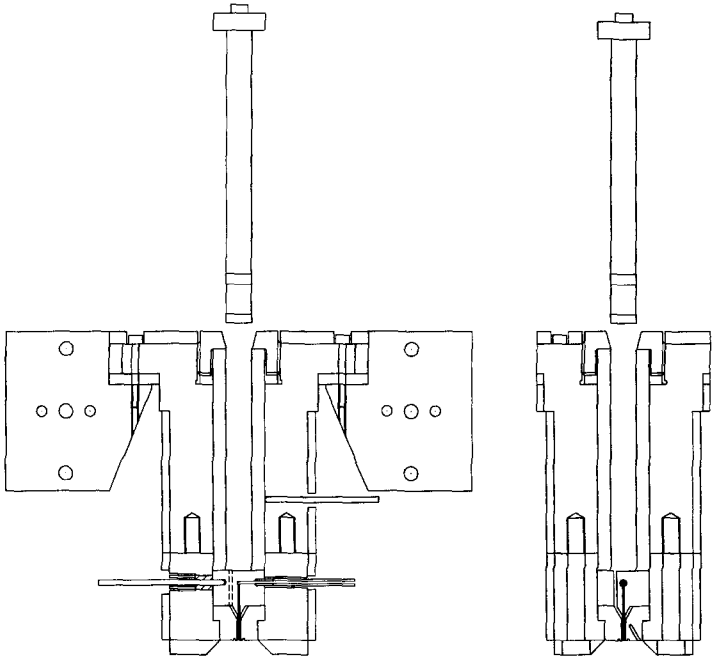

Heating jacket

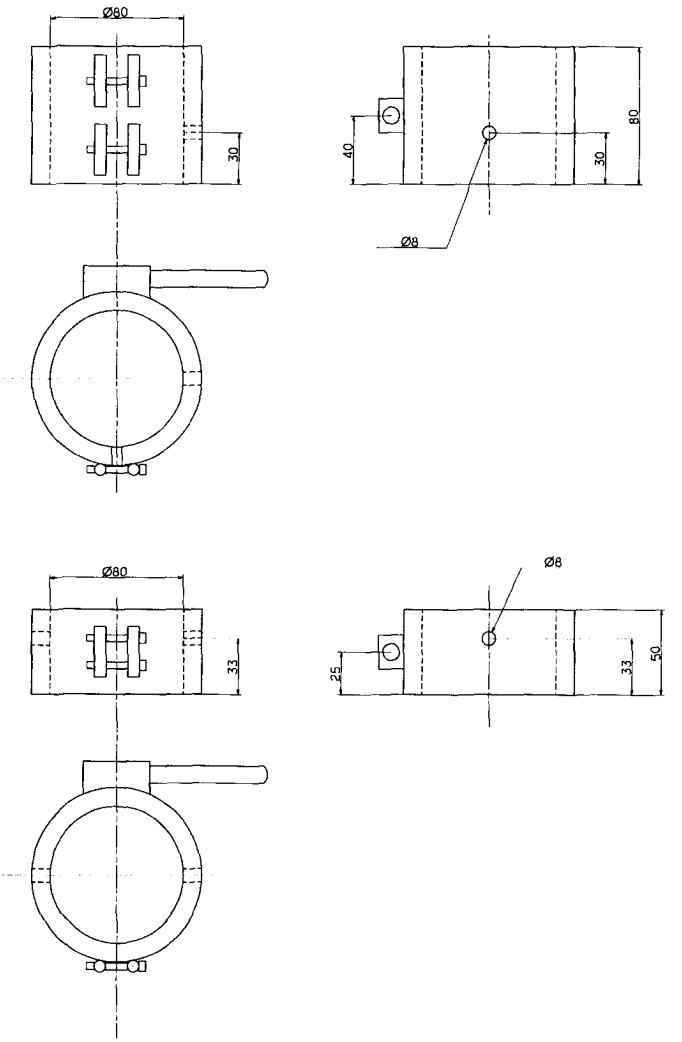

Tube die, for small tube-diameters

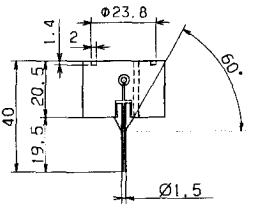

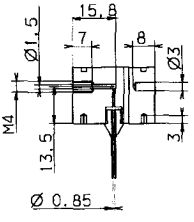

OR 2081 VITON

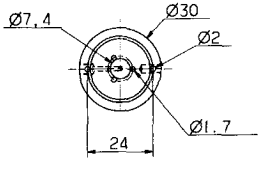

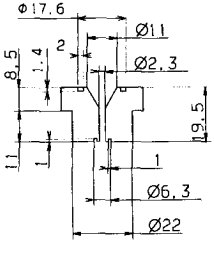

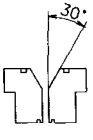

OR 2056 VITON

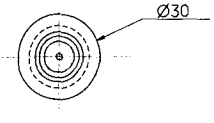

Tube die, for large tube-diameters

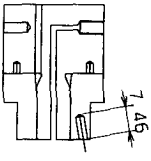

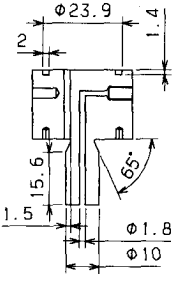

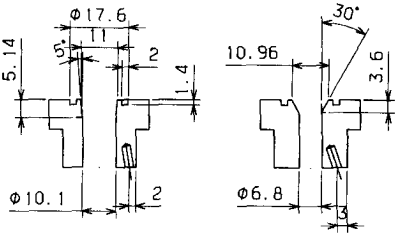

Mat 316L

Mast 1:1

6.12.1996

Cooling nozzle

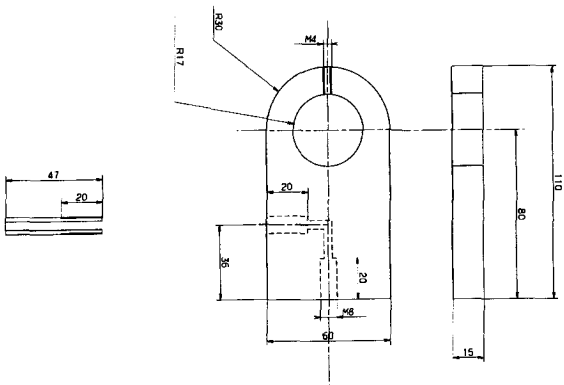

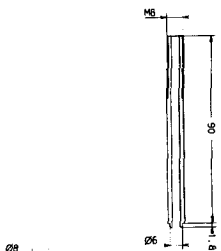

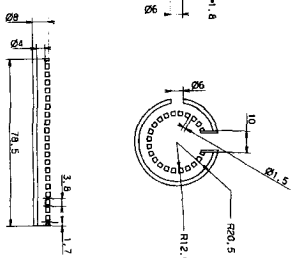

Passive draw-wheel

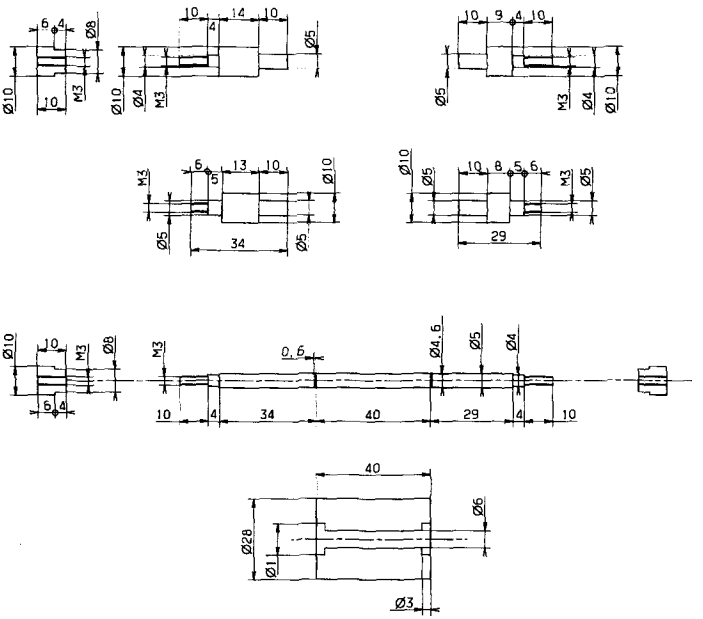

Active draw-wheel

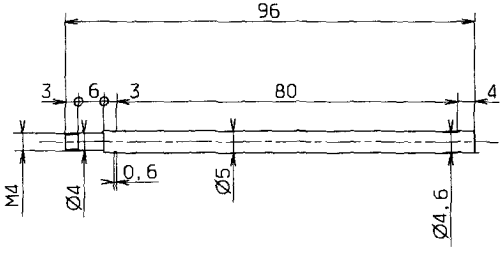

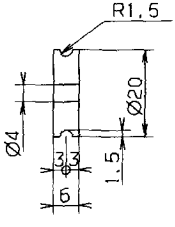

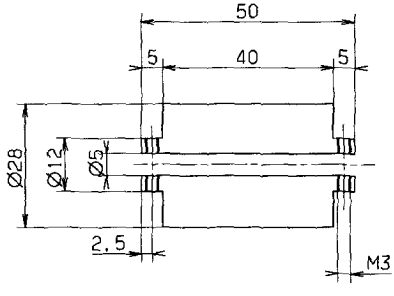

Draw-wheel-lever

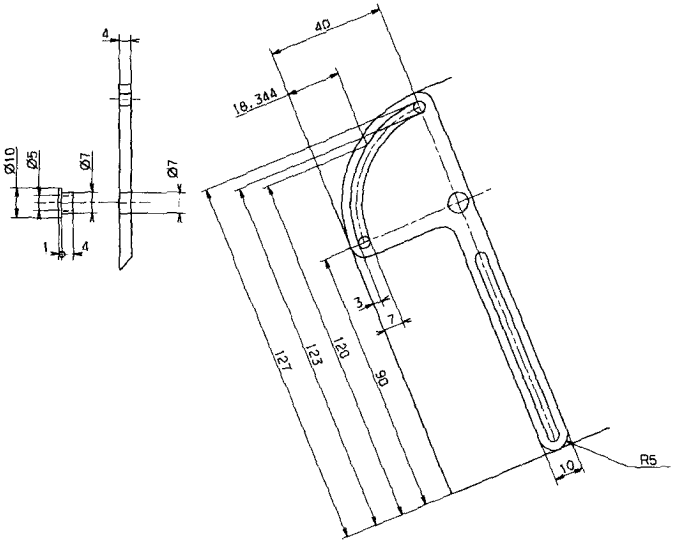

Draw-wheel-block

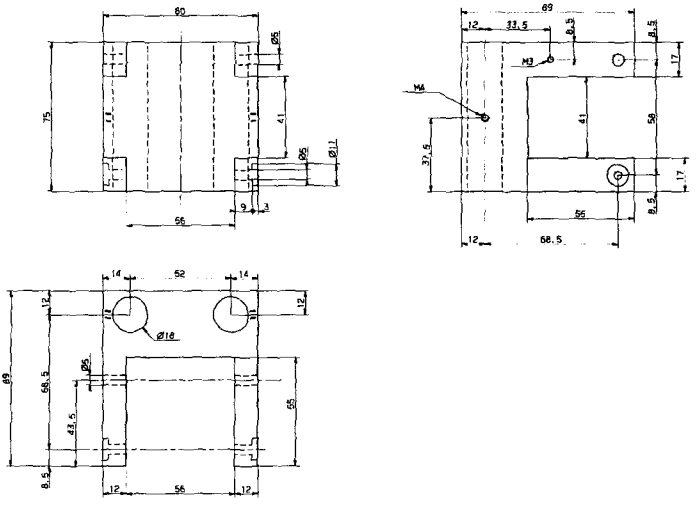

Tube welding rig

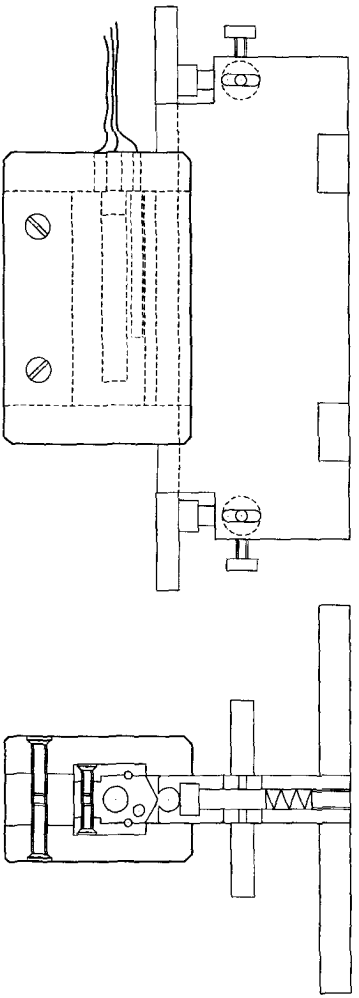

Heating-block of the tube welding rig

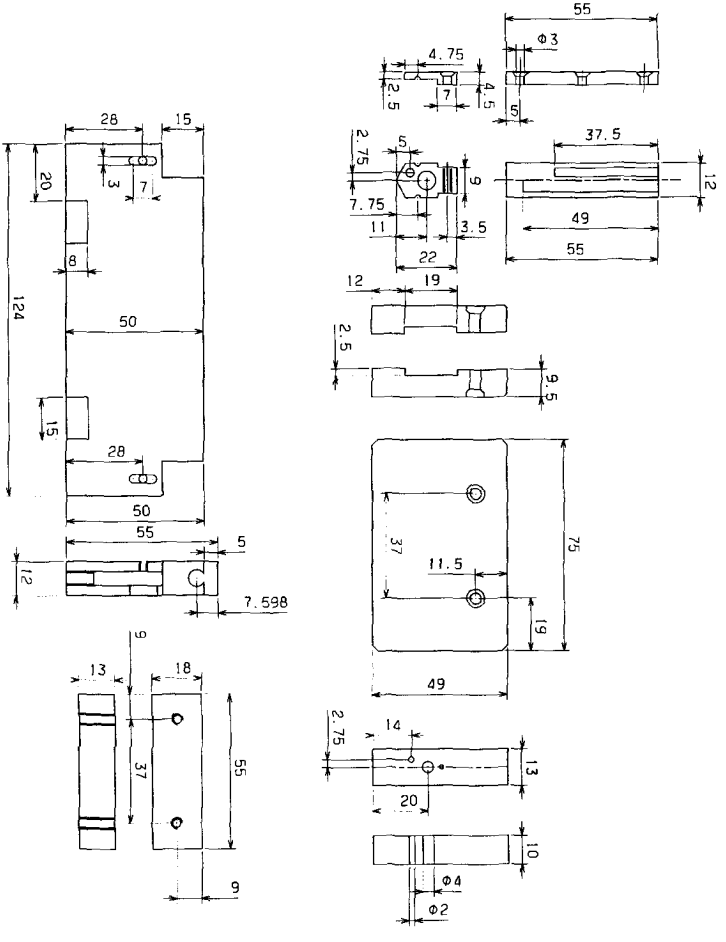

Heating- and cooling device for the x-Ray diffractometer

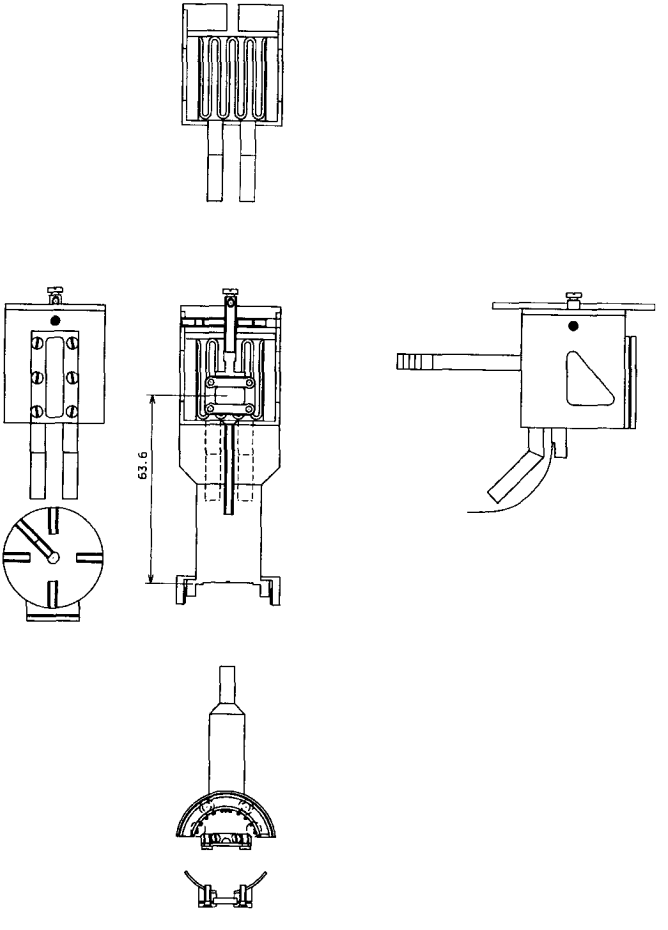

Heating- and cooling device, assembled in a small scale tensile tester